Front. Chem. Sci. Eng. 2022, 16(1): 4–33
https://doi.org/10.1007/s11705-021-2041-2

REVIEW ARTICLE

Recent advances in small molecule fluorescent probes for simultaneous imaging of two bioactive molecules in live cells and *in vivo*

Yongqing Zhou, Xin Wang, Wei Zhang (✉), Bo Tang, Ping Li (✉)

College of Chemistry, Chemical Engineering and Materials Science, Key Laboratory of Molecular and Nano Probes (Ministry of Education), Institutes of Biomedical Sciences, Shandong Normal University, Jinan 250014, China

Abstract The interrelationships and synergistic regulations of bioactive molecules play pivotal roles in physiological and pathological processes involved in the initiation and development of some diseases, such as cancer and neurodegenerative and cardiovascular diseases. Therefore, the simultaneous, accurate and timely detection of two bioactive molecules is crucial to explore their roles and pathological mechanisms in related diseases. Fluorescence imaging associated with small molecular probes has been widely used in the imaging of bioactive molecules in living cells and *in vivo* due to its excellent performances, including high sensitivity and selectivity, noninvasive properties, real-time and high spatial temporal resolution. Single organic molecule fluorescent probes have been successively developed to simultaneously monitor two biomolecules to uncover their synergistic relationships in living systems. Hence, in this review, we focus on summarizing the design strategies, classifications, and bioimaging applications of dual-response fluorescent probes over the past decade. Furthermore, future research directions in this field are proposed.

Keywords bioactive molecules, fluorescent probes, in living cells and *in vivo*, review

1 Introduction

Biological environments maintain homeostasis via multiple intracellular molecular events [1,2]. These processes are controlled by the interactions between various bioactive molecules involved in maintaining health [3]. For example, H_2S and hydrogen polysulfides (H_2S_n) are endogenous regulators of multiple physiological processes [4]. However, abnormal variations in these bioactive molecules are involved in diseases. For example, high reactive oxygen species (ROS) and Fe^{2+} levels have been found in Parkinson's disease (PD) patients [5]. Hence, to explore the relationships and synergistic regulations of bioactive molecules, we must obtain profound insight into intracellular molecular communication. That is, we need to reveal the concentrations, distributions, functions and mechanisms of two intracellular reactive molecules, especially during the progression of related diseases.

Fluorescent probes have been recognized as one of most effective tools for the study of molecular events in biological systems [6,7]. In particular, they greatly facilitate the elucidation of the key roles of metal ions, reactive oxygen/nitrogen/sulfur species, anions and enzymes in live cells and *in vivo* [8–11]. Although dual-detection fluorescent probes based on nanomaterials have been reported recently, their application in bioimaging is limited by complex constructs and poor stability. Compared with nanomaterial probes, small molecule fluorescent probes present significant advantages in the bioimaging field, such as faster diffusion, easier metabolism, low toxicity and few side effects *in vivo* [12–14]. Therefore, single-structure and dual-sensing fluorescent probes are fascinating options for simultaneously imaging two bioactive molecules in live cells and *in vivo*.

To date, the chemical structures of these dual-detection probes have varied considerably, but they usually possess one or more fluorophores moieties and one or more recognition units. The common design strategies of dual-response fluorescent probes mainly focus on the following four types, as shown in Scheme 1: (a) A molecule contains a fluorophore and a recognition group. The two analytes simultaneously react with the same recognition group to generate different fluorescence products. (b) A molecule is

Received November 17, 2020; accepted January 15, 2021

E-mails: zhangwei@sdnu.edu.cn (Zhang W); lip@sdnu.edu.cn (Li P)

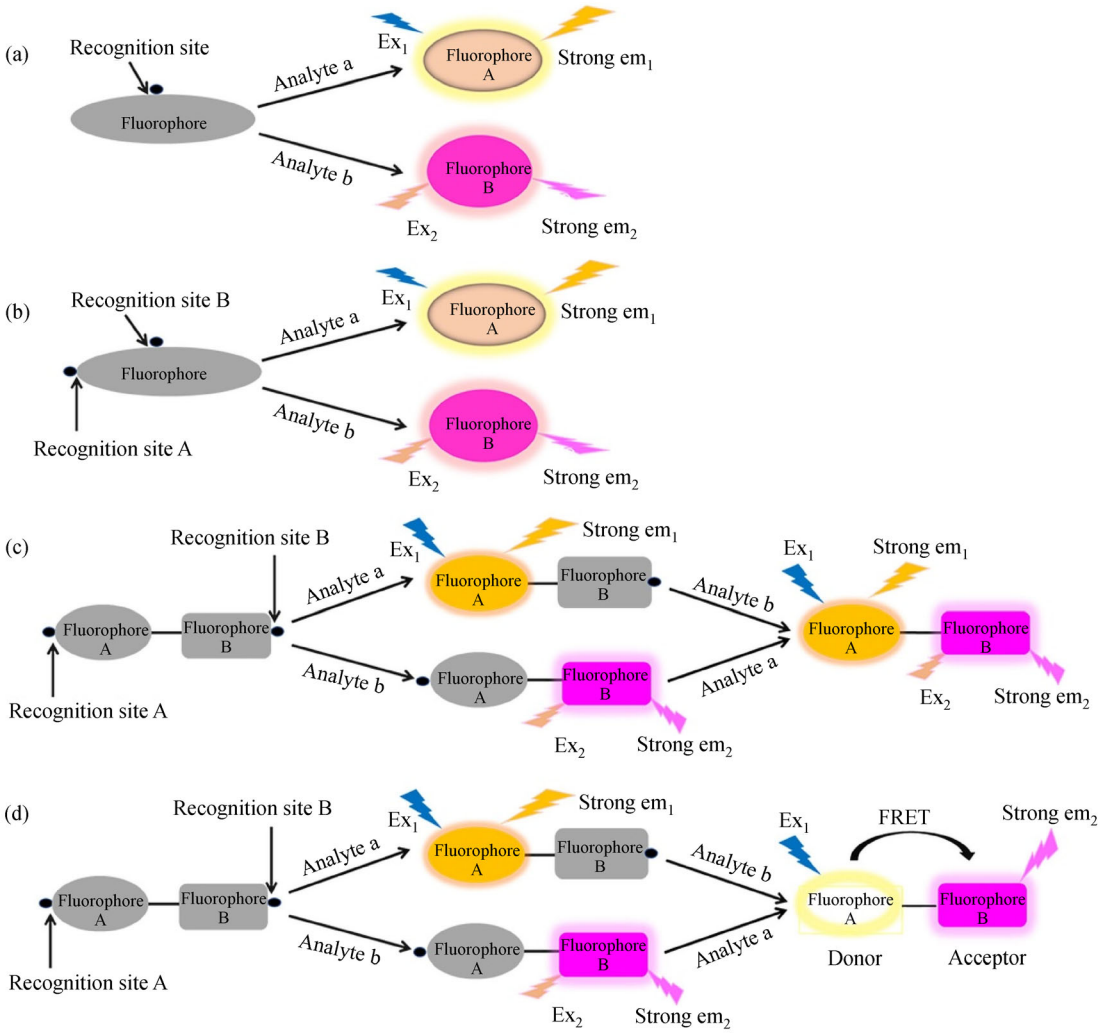

Scheme 1 Design strategies of dual-response fluorescent probes for simultaneously monitoring two reactive molecules.

composed of one fluorophore and two recognition units. The two bioactive molecules respond with the two recognition sites to generate fluorescent products with distinguishable spectra. (c) A molecule possesses two fluorophores and two recognition sites. One specific recognition group responds to a single analyte, producing different fluorescent products with noninterfering spectra. (d) A molecule-based fluorescence resonance energy transfer (FRET) mechanism is constructed [15,16], since the emission spectrum of the donor effectively coincides with the absorption spectrum of the receptor after simultaneously reacting with the two analytes. All these dual-response probes based on the above four design strategies can be used to simultaneously image two analytes in living systems. However, these probes have various advantages and disadvantages in terms of structures and performances. First, compared with those of strategies (c) and (d), the probe structures of strategies (a) and (b) are simple and easy obtained; second, given that fluorescence spectra the discrimination effect of strategy (c) is more significant than that of the other strategies. Hence, the fluorescent probes constructed based on strategy (c) can better detect the two reactive molecules simultaneously. Here, this review will provide a detailed description of dual-response fluorescent probes. Moreover, to better help readers understand the importance of this field, we also classify reported probes that image bioactive molecules simultaneously according to the different bioactive species.

2 Simultaneous imaging of two bioactive molecules

2.1 Simultaneous imaging of two metal ions

Metal ions are key elements for living organisms and serve as an essential catalytic center of various proteins and

enzymes in elaborate processes [17,18]. An abnormal concentration of metal ions is closely related to the pathogenesis of various diseases, including neurodegenerative diseases [19], PD and Alzheimer's disease [20,21]. Currently, to study and dissect the relationships and differences between two metal ions, researchers have developed a variety of organic small fluorescent probes to simultaneously visualize the concentrations, distributions and correlations of some metal ions in cells and *in vivo*, such as Cu^{2+}/Al^{3+}, Zn^{2+}/Al^{3+}, Zn^{2+}/Hg^{2+} and Mg^{2+}/Hg^{2+} (Table 1).

Two fluorescent probes have been successively developed for simultaneous detecting Cu^{2+}/Al^{3+} and Zn^{2+}/Al^{3+} (Fig. 1). For example, a dual-response fluorescent probe ($C_{14}H_{13}N_3O_3$, H_2L) based on a *bis*-Schiff base has been designed by the Shuang group [22]. H_2L possessed nitrogen and oxygen atoms, and provided rich coordination locations for Al^{3+} and Cu^{2+} (Fig. 1(a)). Firstly, the *cis-trans* isomerization of H_2L was inhibited, and H_2L showed weak fluorescence. When Cu^{2+} or Al^{3+} was combined with nitrogen and oxygen atoms under different pH conditions, the fluorescence of H_2L was enhanced due to an increase in rigidity. Therefore, H_2L could simultaneously respond to Cu^{2+} and Al^{3+} ions with different spectral signals (Cu^{2+} at 520 nm, Al^{3+} at 440 nm). These detection limits of H_2L were suitable for the physiological levels of Cu^{2+} and Al^{3+}, respectively. More importantly, H_2L was capable of simultaneously imaging exogenous Al^{3+} and Cu^{2+} in HeLa cells.

The Roy group constructs two fluorescence probes, 2-(2-((3-(*tert*-butyl)-2-hydroxybenzylidene)amino)ethyl)-3-butylbis(ethylamino)-2-ylamidimethylspiro[indoline-1,9[ixanthen]-3-one (HL-*t*-Bu) and 4-methyl-2-((quinolin-2-ylimino)methyl)phenol (2-QMP), for dual-color detection of Zn^{2+} and Al^{3+} through different fluorescence channels [23,24]. HL-*t*-Bu coordinated with Zn^{2+} through the amide bond and salicylaldehyde unit of rhodamine, accompanied by fluorescence intensity enhancement at 457 nm. The open-ring rhodamine could also coordinate with Al^{3+}, causing the fluorescence intensity to increase at 550 nm. Therefore, simultaneous detection of Zn^{2+} and Al^{3+} was achieved through distinguishable fluorescence spectra. Moreover, HL-*t*-Bu showed low biotoxicity and good biocompatibility in living cells, and was successfully applied to study the exogenous level changes of Al^{3+} and Zn^{2+} in mice (Fig. 1(b)). 2-QMP showed low fluorescence due to the photoinduced electron transfer (PET) mechanism [25]. The PET effect of 2-QMP was inhibited after the C = N bond was coordinated with Al^{3+} or Zn^{2+}, which caused strong fluorescence emission at 375 and 550 nm, respectively. Furthermore, 2-QMP was used to image dynamic changes of exogenous Al^{3+} and Zn^{2+} in C6 cells.

The Xu group has developed a multichannel fluorescent probe, multiple turn-on fluorophore (FHCS), which simultaneously differentiates Al^{3+} and Zn^{2+} in living cells [26]. The hydrazine unit of FHCS was efficiently coordinated with Al^{3+} or Zn^{2+} to produce blue or green fluorescence, respectively. Moreover, with increasing concentrations of Al^{3+} or Zn^{2+}, there was a good linear relationship between fluorescence intensity and Al^{3+}/Zn^{2+} concentrations. Importantly, FHCS was successfully used to detect exogenous Al^{3+} and Zn^{2+} in HeLa cells and mice. The Wong group also synthesizes a Schiff base fluorescence sensor (BDNOL) derived from the reaction of pyridinylhydrazine and 4-(diethylamine) salicylaldehyde, which respond more selectively and sensitively to Zn^{2+} and Al^{3+} than other competing metal ions [27]. After coordination with Zn^{2+} and Al^{3+}, the corresponding products emitted bright fluorescence at wavelengths of 575 and 504 nm, respectively. In addition, fluorescence imaging of BDNOL to detect exogenous Zn^{2+} and Al^{3+} in living HeLa cells was further conducted. The experimental results indicated that BDNOL could serve as a potential chemosensor for investigating Zn^{2+} and Al^{3+} in living cells.

The Kocyigit team prepares a new dual channel fluorescent probe (bisphenol A-rhodamine, BAR) that shows a highly selective and sensitive fluorescence response toward Zn^{2+} and Hg^{2+} through two different mechanisms. In the probe, the whole fluorophore was made up of bisphenol and rhodamine, and possessed a binding site with metal ions [28]. Upon the addition of Zn^{2+}, the solution of BAR was caused blue emission by inhibiting excited-state intramolecular proton transfer [29]. However, BAR emitted bright red emission in the presence of Hg^{2+} due to the FRET mechanism. Furthermore, BAR was also used to discover the upregulation of exogenous Hg^{2+} in human prostate cancer cell lines. The Xiao group synthesizes a novel rhodamine-based fluorescent chemosensor (rhodamine derivative, RND), which displays different fluorescence responses toward Hg^{2+} and Mg^{2+} in living systems [30]. In the design strategy, 2-hydroxy-1-naphthaldehyde was linked with rhodamine B to obtain a suitable binding site with different metal ions. After RND bound with Hg^{2+} and Mg^{2+}, RND gave out bright fluorescence at different emission wavelengths of 589 and 523 nm under different excitation wavelengths. More importantly, RND enabled the fluorescence-based visualization of exogenous Hg^{2+} and Mg^{2+} levels in HeLa cells. All these probes have outstanding performances, with high sensitivity and selectivity, a low detection limit, good photostability and low cytotoxicity. Therefore, these works may improve our understanding the relationships between these two metal ions and related diseases.

2.2 Simultaneous imaging of two ROS

ROS include superoxide anion ($O_2\cdot^-$), H_2O_2, hydroxyl radical ($\cdot OH$) single oxygen ($^1O_2$) and HClO, etc. They are the most important biological oxidative species, and play vital roles in intracellular signal transduction pathways,

Table 1 The classifications, chemical structures and applications of fluorescent probes for simultaneously detecting two metal ions

Classification	Chemical structure	Bioactive molecule	Wavelength/nm	Detection limit /(mol·L^{-1})	Application	Ref.
Two metal ions	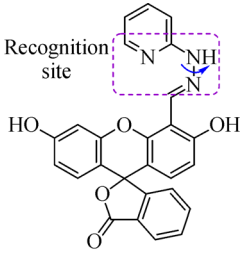 H_2L	Al^{3+} and Cu^{2+}	Al^{3+}: 390/440 Cu^{2+}: 480/520	Al^{3+}: 7.32×10^{-8} Cu^{2+}: 1.47×10^{-8}	In HeLa cells	[22]
	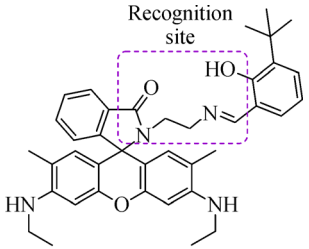 HL-*t*-Bu	Al^{3+} and Zn^{2+}	Al^{3+}: 500/550 Zn^{2+}: 370/457	Al^{3+}: 1.2×10^{-5} Zn^{2+}: 3.6×10^{-5}	In mice	[23]
	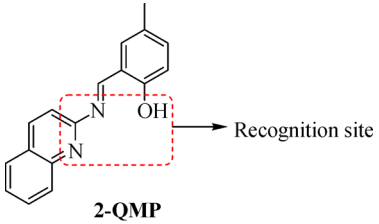 **2-QMP**	Al^{3+} and Zn^{2+}	Al^{3+}: 330/376 Zn^{2+}: 435/550	Al^{3+}: 3.79×10^{-6} Zn^{2+}: 1.363×10^{-7}	In C6 cells	[24]
	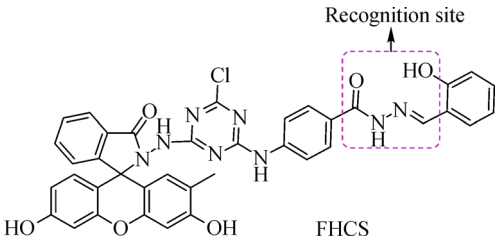 FHCS	Al^{3+} and Zn^{2+}	Al^{3+}: 384/446 Zn^{2+}: 406/500	Al^{3+}: 5.37×10^{-8} Zn^{2+}: 7.9×10^{-8}	In HeLa cells and mice	[26]

(*Continued*)

Classification	Chemical structure	Bioactive molecule	Wavelength/nm	Detection limit /(mol·L^{-1})	Application	Ref.
	Recognition site 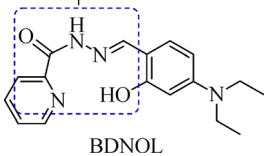 BDNOL	Al^{3+} and Zn^{2+}	Al^{3+}: 390/504 Zn^{2+}: 390/575	Al^{3+}: 8.3×10^{-8} Zn^{2+}: 1.24×10^{-7}	In HeLa cells	[27]
	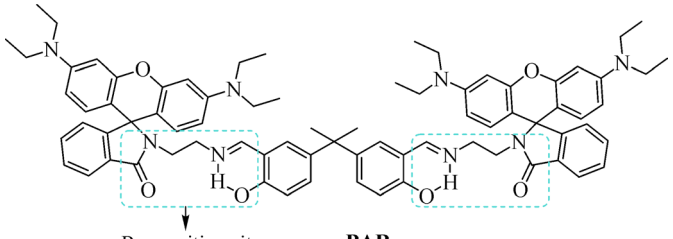 Recognition site **BAR**	Hg^{2+} and Zn^{2+}	Hg^{2+}: 364/580 Zn^{2+}: 364/468	Hg^{2+}: 2.16×10^{-6} Zn^{2+}: 2.21×10^{-6}	In human prostate cancer cell	[28]
	Recognition site 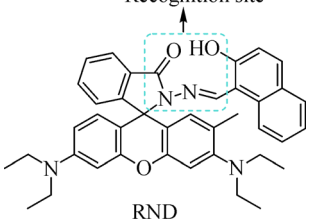 RND	Hg^{2+} and Mg^{2+}	Hg^{2+}: 500/589 Mg^{2+}: 360/523	Hg^{2+}: 8.0×10^{-8} Mg^{2+}: 1.0×10^{-5}	In HeLa cells	[30]

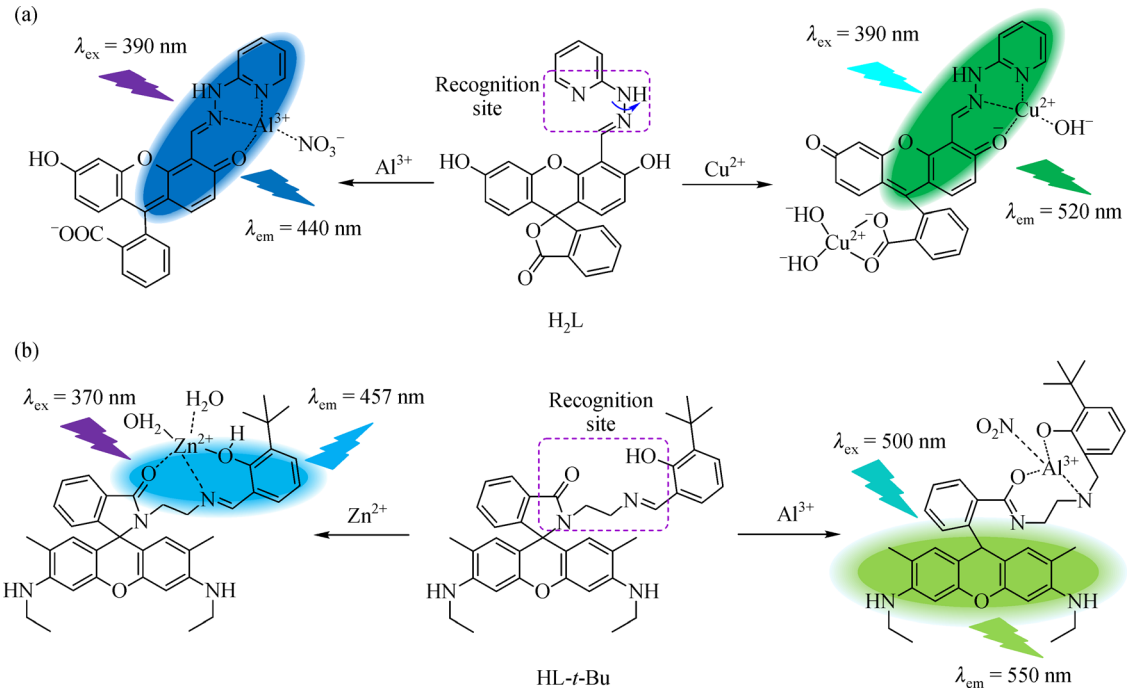

Fig. 1 The chemical structures and corresponding sensing mechanisms of H_2L and HL-*t*-Bu in the presence of two metal ions.

redox equilibrium, and cellular immune and apoptosis processes [31–34]. However, the excessive production of ROS can cause oxidative damage to biomolecules, such as nucleic acids, lipids and proteins, and even lead to the loss of cell function. Importantly, the overproduction of ROS is associated with pathological processes, including aging, reperfusion injury, cancer and cardiovascular diseases [35,36]. Therefore, a series of fluorescent probes have been successively developed for simultaneous imaging to reveal the interrelationships of two ROS in various physiological processes (Table 2).

The Zhang group constructs a single-structure fluorescent probe ($C_{26}H_{26}N_2O_7$, FHZ) for the identification of ·OH and HClO in living organisms [37]. FHZ alternatively used fluorescein as the skeleton, in which was attached with a five-member ring and a triethylene glycol chain (Fig. 2). The two active sites of FHZ quenched the fluorescence of fluorescein, and could react with ·OH and HClO. In the presence of HClO, the hydrazide group was broken and formed an open-loop fluorescein, which emitted an obvious fluorescence signal at 520 nm. In the presence of ·OH, the phenol structure was also destroyed and emitted strong fluorescence at 486 nm (Fig. 2(a)). Moreover, FHZ was successfully used to monitor exogenous and endogenous ·OH and HClO levels in RAW264.7 cells under different time and stimulation conditions (Figs. 2(b) and 2(c)), owing to its water solubility, real-time visualization and good biocompatibility. In particular, FHZ was employed to visualize ·OH in living zebrafish for the first time. Hence, FHZ will act as a powerful platform to study the related functions and mechanisms of different ROS in living organisms.

The Wang group reports a new dual-site fluorescence imaging probe (Geisha-1) based on a FRET platform to identify HClO or H_2O_2 [38]. In this FRET platform, coumarin was chosen as the FRET donor, and naphthalimide was chosen as the FRET acceptor. These fluorophores were linked to the corresponding recognition groups of dimethylthiocarbamate and borate, respectively. With the addition of H_2O_2 or HClO, the boronate bond or dimethylthiocarbamate group was cleaved and released the 1,8-naphthalimide or coumarin dye, which turned on fluorescence at 550 or 452 nm. When H_2O_2 and HClO coexisted in solution, the emission spectrum of coumarin overlapped with the absorption spectrum of 1,8-naphthalimide, leading to an effective FRET process due to the suitable distance. Bright fluorescence was observed in living cells and liver tissues in the presence of exogenous HClO and H_2O_2. Wang's team also reports a fluorescent probe (CSU1) for investigating the relationships between H_2O_2 and HClO with two distinct fluorescence channels [39]. CSU1 contained a phenothiazine-based coumarin dyad and two recognition units, an HClO-responsive phenothiazine and an H_2O_2-sensing boronate ester. Upon the addition of HClO, the "S" atom of CSU1 was oxidized to sulfoxide, and obtained a new structure with an internal charge transfer (ICT) effect [40], thereby resulting in a fluorescence change from red to green. The boronate unit was cleaved with H_2O_2 and released phenothiazine-based coumarin with red fluorescence. Moreover, CSU1 was

Table 2 The classifications, chemical structures and applications of fluorescent probes for simultaneously detecting two ROS

Classification	Chemical structure	Bioactive molecule	Wavelength/nm	Detection limit/(mol·L^{-1})	Application	Ref.
Two ROS	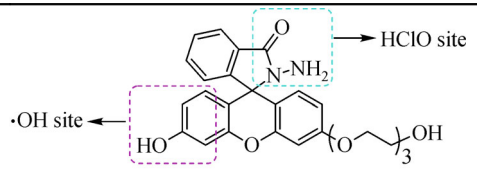 FHZ	·OH and HClO	·OH: 410/496 HClO: 490/520	–	In RAW264.7 cells and zebrafish	[37]
	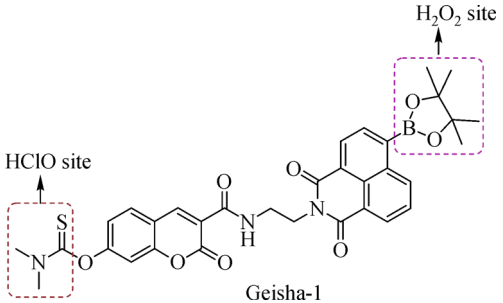 Geisha-1	H_2O_2 and HClO	H_2O_2: 450/550 ClO^-: 400/452	H_2O_2: 6.46×10^{-8} ClO^-: 2.82×10^{-8}	In cells and liver tissue	[38]
	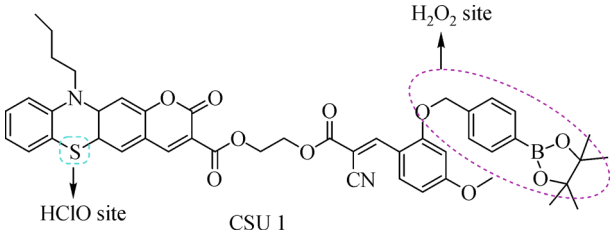 CSU 1	H_2O_2 and HClO	H_2O_2: 376/409, 376/640 HClO: 440/520, 440/640	H_2O_2: 1.5×10^{-8} HClO: 1.3×10^{-8}	In MCF-7 cells	[39]
	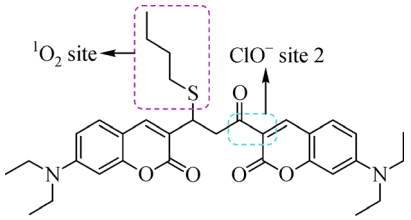 Hy-1	$^1O_2$ and HClO	$^1O_2$: 420/475 ClO^-: 480/526	$^1O_2$: 3.5×10^{-7} ClO^-: 5.3×10^{-8}	In HepG2 cells and in mice	[41]

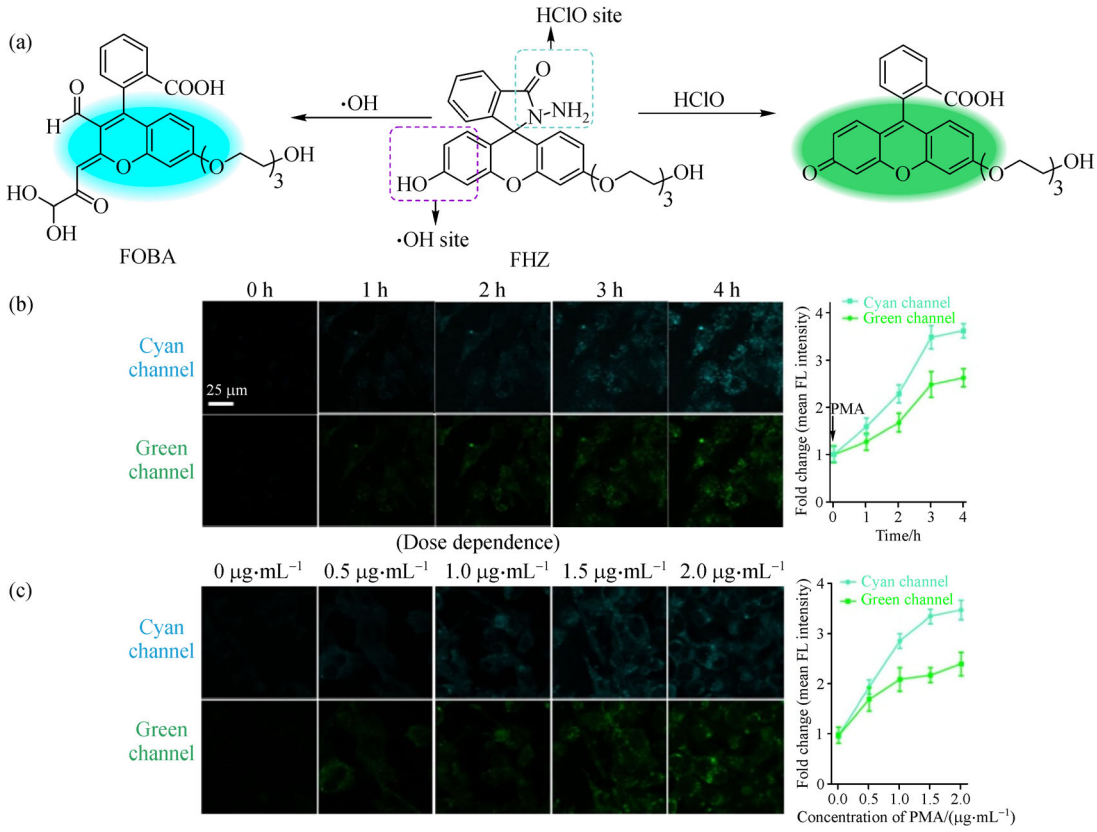

Fig. 2 (a) Chemical structure and recognition mechanism of FHZ; (b) and (c) confocal microscopy fluorescence imaging of FHZ in RAW264.7 cells under different time and stimulation conditions. Reprinted with permission from Ref. [37], copyright 2016 American Chemical Society.

successfully utilized to distinguish H_2O_2 and HClO through different ratios of fluorescence signals. Importantly, CSU1 could also clearly monitor endogenous generation of HClO from H_2O_2 and Cl^- catalyzed by myeloperoxidase in MCF-7 cells.

The Wang group fabricates the first dual-functional fluorescent probe (Hy-1) for simultaneous ratiometric imaging of ClO^- and $^1O_2$ with high sensitivity and selectivity [41]. In the presence of HClO, the thioether moiety of Hy-1 was oxidized, and a coumarin with strong ICT effect was formed. The fluorescence was reduced at 475 nm and enhanced at 526 nm after Hy-1 responded to ClO^-. $^1O_2$ oxidized the thioether bond to form the whole conjugated product, and the fluorescence was reduced at 475 nm and enhanced at 597 nm. Furthermore, Hy-1 could also accumulate in mitochondria, which makes Hy-1 an effective tool for monitoring exogenous and endogenous ClO^- and $^1O_2$ levels in human hepatocellular liver carcinoma (HepG2) cells. Significantly, the fluorescence imaging study with this Hy-1 revealed that the levels of ClO^- and $^1O_2$ were upregulated in the deep cecum tissue of mice with polymicrobial sepsis. This work provides a robust strategy to explore the signaling and oxidative pathways related to two ROS, and is widely applied in the field of biological diagnosis.

2.3 Simultaneous imaging of two reactive sulfur species (RSS)

RSS are a class of reductive species that include glutathione (GSH), cysteine (Cys), homocysteine (Hcy), H_2S and H_2S_n. These species are closely linked to complex redox equilibrium and scavenging of toxins in living organisms [42–44]. The abnormal levels of RSS have been identified as an indicator of many diseases, including cancer, neurodegenerative diseases, and liver damage [45,46]. In the past decade, to illuminate the biological effects and crosstalk of two different RSS, some fluorescence imaging tools have been developed to accurately and synchronously detect RSS (Table 3).

The Guo group prepares two fluorescent probes (OP and POP)-based pyronin dyes to simultaneously visualize the mutual interconversion between Cys and GSH by substitution-rearrangement and substitution reactions [47]. Through green and red fluorescence channels, POP displayed better performances than OP in dual-response

Table 3 The classifications, chemical structures and applications of fluorescent probes for simultaneously detecting two RSS

Classification	Chemical structure	Bioactive molecule	Wavelength/nm	Detection limit/(mol·L^{-1})	Application	Ref.
Two RSS	Recognition site OP:R = H POP: R = PPh_2	Cys and GSH	Cys: 450/545 GSH: 580/620	–	In living cells and in mice	[47]
	Recognition site 3o	Cys and GSH	Cys: 480/529 GSH: 480/550	–	In HeLa cell	[48]
	Site 1, Site 2, Site 3 Probe 1 (Guo group)	Cys and GSH	Cys: 360/420 GSH: 450/512	GSH: 5.0×10^{-8}	In COS-7 cells	[49]
	Site 1, Site 2, Site 3 **QB-3**	Cys and GSH	Cys: 365/420 GSH: 495/537, 495/643	Cys: 1.7×10^{-7} GSH: 4.6×10^{-7}	In HepG2 cells	[50]
	Site 1, Site 2 Probe 1 (Zhang group)	H_2S and GSH	H_2S: 515/564 GSH: 430/517	H_2S: 4.2×10^{-8} GSH: 8.7×10^{-8}	In MCF-7 cells	[51]

(*Continued*)

Classification	Chemical structure	Bioactive molecule	Wavelength/nm	Detection limit/(mol·L^{-1})	Application	Ref.
	Site 1, Site 2 Probe 1 (Yin group)	H_2S and GSH	H_2S: 510/587 GSH: 430/501	H_2S: 2.855×10^{-5} GSH: 7.55×10^{-6}	In RAW cells	[52]
	H_2S_n site, H_2S site **DDP-1**	H_2S and H_2S_n	H_2S: 360/452 H_2S_n: 515/542	H_2S: 1.5×10^{-7} H_2S_n: 2.4×10^{-8}	In HeLa cells	[4]
	H_2S site, H_2S_n site MC-Sn	H_2S and H_2S_n	H_2S: 410/519, 410/606 H_2S_n: 410/468, 410/606	H_2S: 3.4×10^{-8} H_2S_n: 2.1×10^{-8}	In RAW264.7 cells	[53]
	HSO_3^- site, Biothiols site CZ-BZ-CHO	HSO_3^- and biothiols	Cys: 497/590 HSO_3^-: 350/445, 350/590	Cys: 8.18×10^{-6} HSO_3^-: 7.22×10^{-6}	In HeLa cells	[54]
	SO_2 site, Biothiol site R_1: H, NO_2 R_2: H, NO_2 Probe (Yu group)	SO_2 and biothiols	SO_2: 390/495 Biothiols: 556/665	SO_2: 6.0×10^{-8} Biothiols: 2.02×10^{-7}	In HeLa cells	[55]

(*Continued*)

Classification	Chemical structure	Bioactive molecule	Wavelength/nm	Detection limit/(mol·L^{-1})	Application	Ref.
	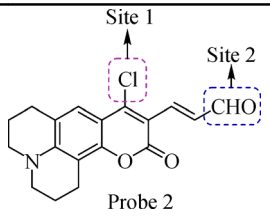 Probe 2	Cys and Hcy	Cys: 400/480 Hcy: 452/542	Cys: 1.99×10^{-6} Hcy: 6.1×10^{-7}	In living cells	[56]
	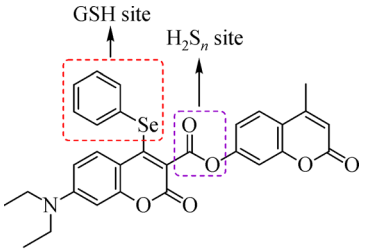 ACC-SePh	GSH and H_2S_n	GSH: 430/540 H_2S_n: 366/465	GSH: 5.6×10^{-8} H_2S_n: 4.0×10^{-8}	In RAW264.7 cells	[57]
	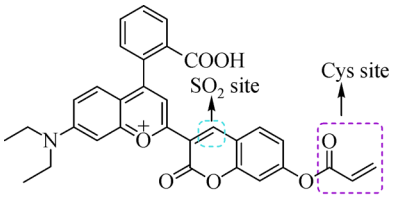 NIR-Cys	Cys and SO_2	Cys: 460/550, 460/664 HSO_3^-: 470/560	Cys: 3.0×10^{-8} HSO_3^-:1.1×10^{-8}	In MCF-7 cells	[58]
	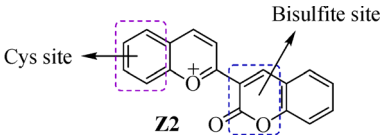 **Z2**	Cys and bisulfite	Cys: 570/640 HSO_3^-: 450/540, 450/640	Cys: 2.0×10^{-8} HSO_3^-: 3.0×10^{-9}	In MCF-7 cells, zebrafish and mice	[59]
	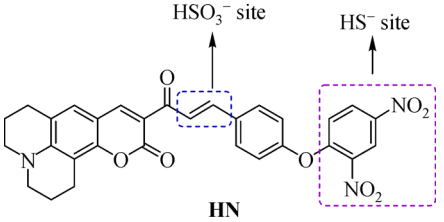 **HN**	HS^- and HSO_3^-	HS^-: 500/581 HSO_3^-: 460/515	HS^-: 1.2×10^{-7} HSO_3^-: 2.0×10^{-8}	In HepG2 cells and LO-2 cells	[60]

fluorescence identification of Cys and GSH (Fig. 3). Furthermore, POP was successfully used for simultaneous differentiation of Cys and GSH concentrations between normal cells and various cancer cells. Moreover, *in vivo* results manifested that distinctly higher biothiol levels in a tumor xenograft nude mouse model than in normal mice. The Hao group has synthesized a class of fluorescence probe-based borondipyrromethene (BODIPY) dyes for selective biothiol detection in HeLa cells [48]. In these probes, the sulfonyl group was introduced as the BODIPY core and leaving group. Moreover, the 2,4-dinitrobenzenesulfonyl group substituted with BODIPY exhibited markedly quenched fluorescence via the PET pathway. Among these probes, 3o had the ability to distinguish Cys and GSH due to various reaction processes. For example, 3o produced bright green fluorescence at 529 nm in the presence of Cys. Conversely, the solution of 3o emitted brilliant yellow light upon the addition of GSH at 550 nm. Importantly, 3o could effectively differentiate various levels of GSH and Cys in HeLa cells by changes in diverse fluorescence intensities. The Guo group also constructs fluorescent probe 1 with three specific reaction sites, which could synchronously identify intracellular Cys and GSH [49]. In probe 1, hemicyanine was attached to coumarin as a complete conjugated structure, with multiple reaction sites (1, 2 and 3) for Cys and GSH. In the case of Cys, nucleophilic substitution occurred at site 1 and site 2 of probe 1 to generate 4a compound. In this case, the whole conjugated structure was interrupted and emitted a bright fluorescence signal (53 times) at 420 nm. In the presence of GSH, site 1 and site 3 were attacked to ultimately produce a new product, with strong fluorescence (67 times) at 512 nm. Probe 1 was able to simultaneously detect increases in exogenous Cys and GSH in African green monkey kidney fibroblast (COS-7) cells according to multicolor spectra. The Song research group has constructed three fluorescent probes based on quinolones for distinguishing both Cys and GSH in two separate fluorescence channels [50]. In these probes, the "Cl" atom was used as the recognition site of biothiols by nucleophilic substitution and intramolecular cyclization reaction. Among them, quinolone-based fluorescent probe (QB-3) possessed the preferred sensing performance for Cys and GSH *in vitro*. Importantly, QB-3 discriminated exogenous Cys and GSH in living HepG2 cells due to its low biotoxicity and good biocompatibility. Altogether, these works offer a class of valuable tools for monitoring Cys and GSH, and have considerable potential applications in cells and *in vivo*.

The Zhang group has developed a dual-channel fluorescent probe 1 that can simultaneously detect changes in GSH and H_2S levels [51]. Probe 1 used coumarin as the fluorophore, the "Cl" atom as an easy leaving moiety and cyano as a quencher owing to its strong electrophilic ability. Upon treatment with GSH or H_2S, new fluorescence peaks were observed at 564 or 517 nm, respectively. Therefore, probe 1 was successfully applied in MCF-7 cells for simultaneous visualization of endogenous GSH and H_2S. The Yin group also reports a new probe based on a steric resistance reaction that simultaneously differentiates GSH and H_2S [52]. This probe used coumarin as the fluorophore and α,β-unsaturated ketone as the recognition unit. Probe produced green or yellow fluorescence emission in the presence of GSH and H_2S, respectively. Furthermore, it had excellent performances, such as stability, selectivity, sensitivity and low toxicity. Using this probe, the upregulation of exogenous GSH and H_2S were observed in RAW264.7 cells and in mice.

To reveal the intertwined roles of H_2S and H_2S_n in some diseases, the Xian group synthesizes a FRET-based fluorescent probe (DDP-1) for the dual detection of H_2S and H_2S_n with different fluorescence spectra [4]. In this design, a coumarin/rhodamine dyad was structured as the core in a FRET system. The azide and phenyl 2-(benzoylthio) benzoate based DDP-1 exhibited specific recognition for H_2S and H_2S_n (Fig. 4). When DDP-1 reacted with H_2S, the azide was reduced to an amino group, and a coumarin with a strong "push-pull" structure was generated. When excited at 360 nm, coumarin exhibited an appreciable fluorescence enhancement at 452 nm. After treatment with H_2S_n, DDP-1 adopted a rhodamine structure with green fluorescence. When H_2S_n and H_2S coexisted, the FRET effect occurred between coumarin and rhodamine, since coumarin and rhodamine could function as donor and acceptor, respectively. Under

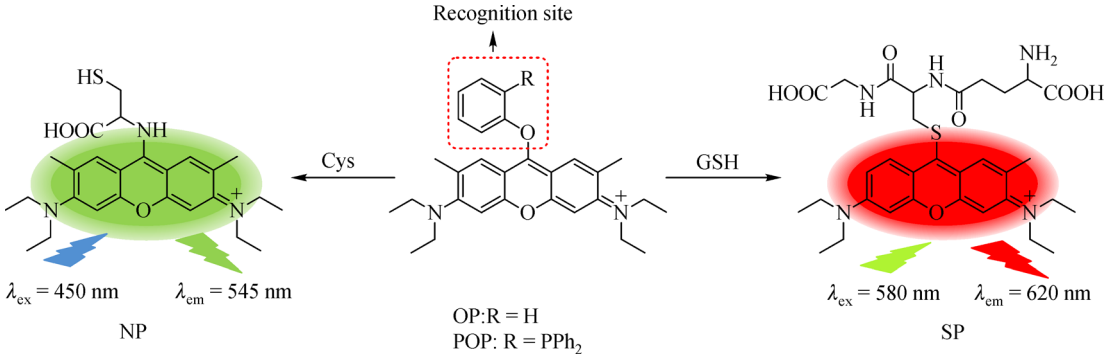

Fig. 3 The chemical structures and recognition mechanisms of OP and POP.

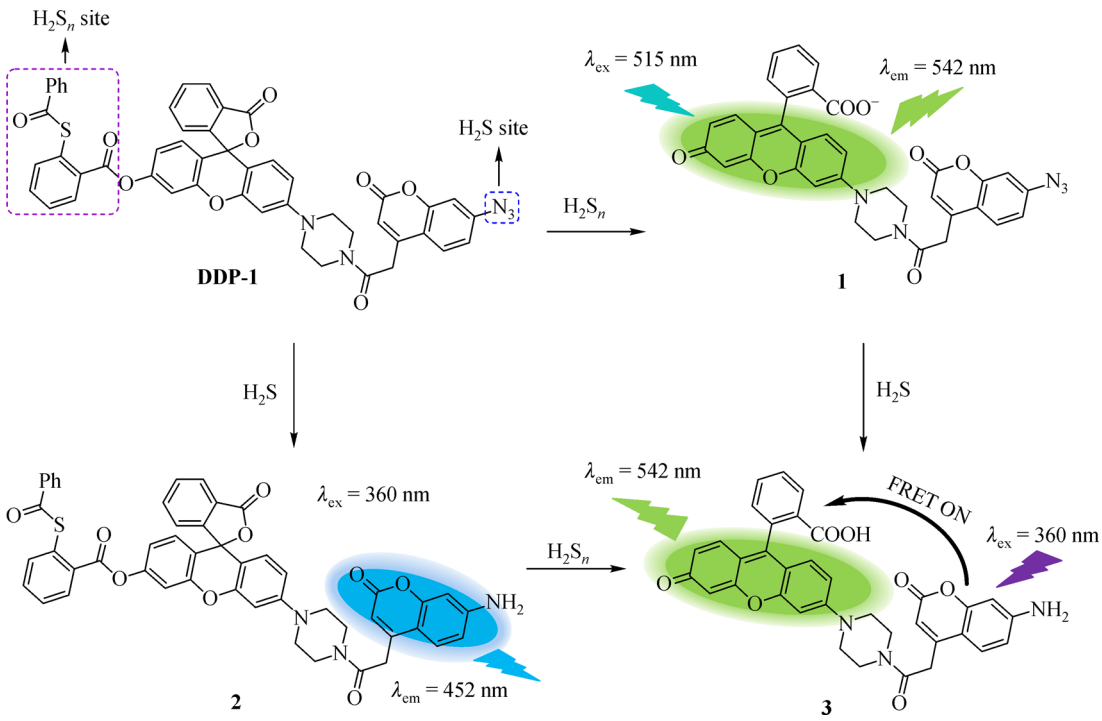

Fig. 4 The chemical structure of FRET-based DDP-1 that facilitates the detection of H_2S_n and H_2S.

excitation at 360 nm, DDP-1 emitted strong fluorescence at 542 nm in the presence of H_2S_n and H_2S. Moreover, DDP-1 effectively measured the increase of exogenous H_2S_n and H_2S in HeLa cells. Subsequently, the Qi research group also reports a novel fluorescent probe (MC-Sn) for the imaging of H_2S and H_2S_n with different spectral channels [53]. In this probe, a near-infrared (NIR) fluorophore was fabricated with naphthol and benzoindole. Moreover, 2-fluoro-5-nitrobenzoic ester was used as both a fluorescence quencher and recognition group of H_2S_n. The intermediate C = C bond was utilized as the nucleophilic reaction site of H_2S. The fluorescence intensity was reduced at 606 nm, accompanied by the addition of H_2S and H_2S_n. However, the fluorescence intensity of the corresponding products was enhanced at 519 and 468 nm. Therefore, MC-Sn could serve as a ratiometric imaging tool for H_2S or H_2S_n. Given that MC-Sn had low biotoxicity and favorable biocompatibility, it was successfully applied in imaging analysis of exogenous H_2S_n in RAW264.7 cells. Particularly, with the advantage of two-photon deep imaging properties, MC-Sn was employed to disclose the upregulation of exogenous H_2S and H_2S_n in the deep tissues of zebrafish and mice.

The Yu group reports a fluorescent probe, CZ-BZ-CHO, for the simultaneous detection of biothiols and sulfite (HSO_3^-), with dual specific sulfide recognition sites [54]. CZ-BZ-CHO used an aldehyde group as the identification site of biothiols and C = C as the nucleophilic addition site of HSO_3^-. In the presence of biothiols or HSO_3^-, bright red fluorescence at 590 nm or blue fluorescence at 445 nm was emitted, respectively. CZ-BZ-CHO showed the characteristics of high selectivity and good biocompatibility, and could monitor the increase in HSO_3^- levels in HeLa cells stimulated with *N*-ethylmalebutenimide. The Yu team also reports an NIR fluorescent probe (BPO-Py-diNO_2) for the detection of biothiols and SO_2 in lysosomes [55]. BPO-Py-diNO_2 used chromenylium with high quantum yield as the NIR fluorophore, the C = C double bond as the recognition site of SO_2, and the pyridine derivative with strong electron-withdrawing group, as well as the biothiol recognition site. Moreover, the BPO-Py-diNO_2 could selectively aggregate in lysosomes. With the two advantages of NIR and a large wavelength shift, the aim of simultaneous differentiation between SO_2 and GSH was realized. Importantly, BPO-Py-diNO_2 enabled fluorescence visualization of exogenous SO_2 level in HeLa cells.

The Liu group has developed fluorescent probe 2 based on a cascade reaction, which can simultaneously distinguish Cys and Hcy via noninterfering emission spectra [56]. In this design strategy, the "Cl" atom and α,β-unsaturated aldehyde group were used as two recognition sites, which were attacked by Cys and Hcy to generate different fluorescent products. Moreover, taking advantage of its high selectivity and good biocompatibility, this probe 2 had been successfully used to differentiate Cys and Hcy in normal cells and some cancer cells.

The Song group reports a fluorescent probe (ACC-SePh) for dual-color monitoring of GSH and H_2S_n [57]. As shown in Fig. 5, the phenylselenide moiety was served as a leaving group in the probe, as well as an effective fluorescence quencher due to the PET mechanism. After

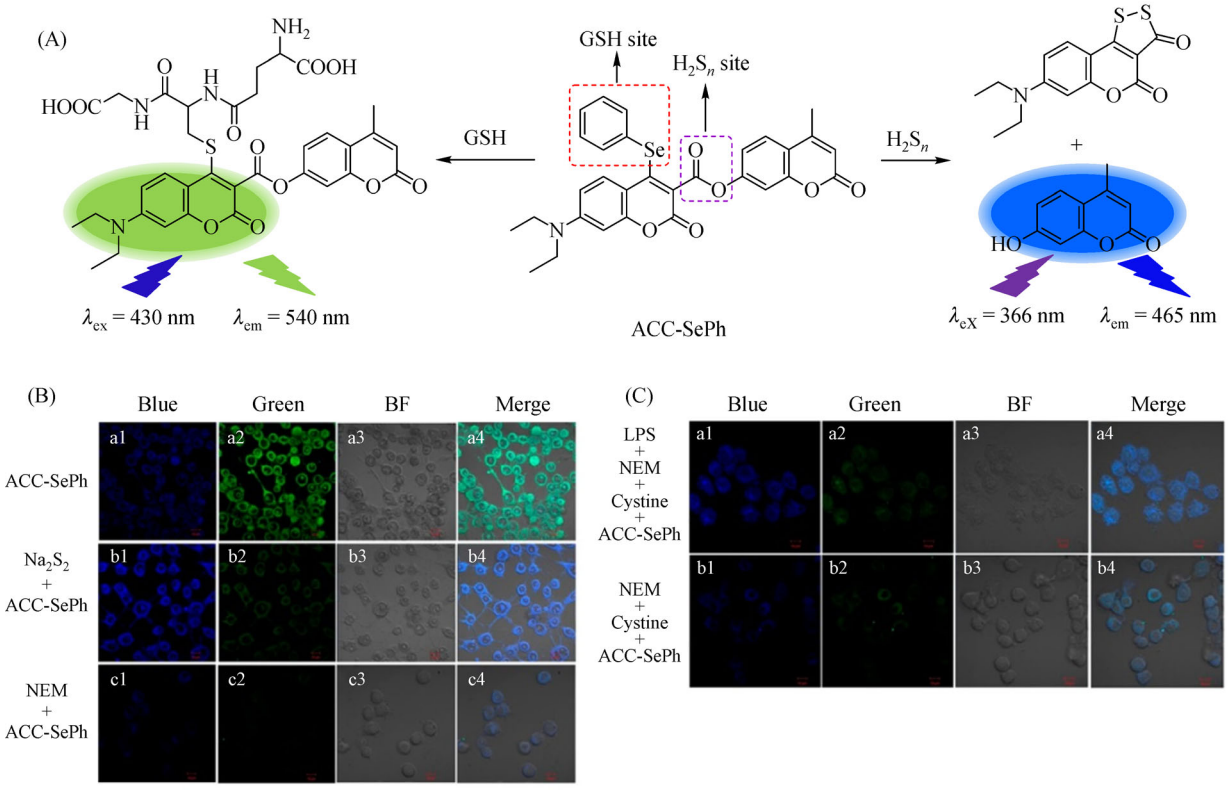

Fig. 5 (A) The proposed sensing mechanism of ACC-SePh for monitoring H_2S_n and GSH; (B) fluorescence imaging of GSH and H_2S_n in living RAW264.7 cells; (C) fluorescence imaging of endogenously produced H_2S_n in living RAW264.7 cells. Reprinted with permission from Ref. [57], copyright 2017 American Chemical Society.

the reaction with H_2S_n, a new fluorescence peak emerged at 465 nm. The addition of GSH brought a new fluorescence emission at 540 nm (Fig. 5(A)). Moreover, ACC-SePh possessed distinguishable emission peaks when GSH and H_2S_n coexisted *in vitro*. Moreover, ACC-SePh displayed high selectivity for GSH and H_2S_n over other common active sulfur substances, such as Cys, Hcy and H_2S. Significantly, ACC-SePh could also be used for in-depth studying of the biological function of GSH and H_2S_n in living RAW264.7 cells (Figs. 5(B) and 5(C)).

Ye's research group has prepared a ratiometric and two-channel fluorescent probe (near infrared-Cys, NIR-Cys) that detected SO_2 and Cys simultaneously [58]. In the structural design, the coumarin group was attached to benzofuran as the whole fluorophore, and the acrylate and C = C moieties of the coumarin were utilized as the recognition groups for Cys and SO_2, respectively. With the addition of Cys, the acrylate unit was degraded, and the NIR fluorophore was generated. In addition, a nucleophilic addition reaction occurred between SO_2 and C = C, leading to destroy the conjugated structure, eventually releasing the benzofuran chromophore. Cell fluorescence imaging suggested that NIR-Cys selectively stained in mitochondria. Owing to the advantages of NIR excitation and emission, NIR-Cys was successfully employed in simultaneous visualization of Cys and SO_2 metabolism in cells, zebrafish and mice. This group rationally designed a mitochondrion-targeting NIR fluorescence probe (Z2) for the simultaneous detection of Cys and bisulfite [59]. Z2 consisted of coumarin and benzopyrylium dye linked by a single bond. These response units for Cys and bisulfite were located on these fluorophores. After Z2 responded to Cys and HSO_3^-, fluorescence was enhanced at 640 and 540 nm, respectively. Z2 showed high selectivity, anti-interference and quick response. Hence, Z2 was widely used for simultaneous imaging of Cys and HSO_3^- in MCF-7 cells, zebrafish and mice.

The Yin group rationally constructs a dual-response fluorescent probe (HN) for studying the metabolic pathways of Cys in cells and zebrafish [60]. In design strategy, coumarin was selected as fluorophore, and the α,β-unsaturated C = C and 2,4-dinitrophenyl moieties were connected as the sensitive reaction sites of HSO_3^- and HS^-, respectively. After HN reacted with HSO_3^- and HS^-, two new fluorescence peaks with an appropriate distance (66 nm) were observed. Moreover, HN could distinguish HSO_3^- and H_2S levels in normal human hepatocyte (LO-2) cells and HepG2 cells via different fluorescence responses. Overall, HN could real time track the metabolic process of H_2S and SO_2 under physiological conditions. These above

tools could help to explore the new role of RSS in living systems and cellular signaling. There novel strategies can serve as useful tools to understand the redox signaling, metabolic processes and signaling pathways of intracellular RSS.

2.4 Simultaneous imaging of one ROS and one RSS

Sometimes, ROS and RSS synergistically regulate signal transmission and redox homeostasis processes in cells and *in vivo* [61,62]. A variety of highly selective and sensitive fluorescent probes have been developed for the simultaneous detection of ROS/RSS to study corresponding concentration fluctuations in living cells and *in vivo* (Table 4). For example, the Ye group reports a fluorescent probe (NPClA) based on a dual-response site and three-signal readouts, that simultaneously monitors SO_2 and HClO level changes in mitochondrial [63]. NPClA was constructed by linking two fluorescence dyes, pyrazoline and semicyanine (Fig. 6). Nitrogen cations helped NPClA accumulate in mitochondria. In the presence of SO_2, a nucleophilic addition reaction occurred at the C = C bond and interrupted the conjugated structure, emitting significant fluorescence at 482 nm. In the presence of HClO, pyrazoline was partially oxidized to produce fluorescence signals at 425 and 585 nm. The probe revealed that the contents of HClO and H_2S were simultaneously enhanced in mitochondria under lipopolysaccharide (LPS)-induced oxidative stress. Subsequently, the You group also has synthesized a two-color fluorescent probe, 2-(4-(1-methylphenanthro-9,10-imidazole-2-yl)-benzylidene) malononitrile (MPIBA), which was used for simultaneous imaging detection of SO_2 and HClO [64]. Modified phenanthroimidazole was introduced as the fluorophore, and malononitrile was introduced as the two reaction sites of SO_2 and ClO^-. The reaction between MPIBA with SO_2 and ClO^- generated different products, which caused fluorescence emission from 625 to 410 and 500 nm, achieving simultaneous differentiation of SO_2 and ClO^- by a ratiometric imaging model. On the basis of these results, MPIBA realized simultaneous ratio imaging of exogenous and endogenous SO_2 and HClO in HeLa cells and zebrafish. To realize ratiometric imaging of SO_2 and HClO in mitochondria, this group also constructs a probe ($C_6H_4N_2O_4$, DNB) with desirable two-photon and ratiometric properties [65]. In the design, naphthalene was selected as the fluorophore, and malononitrile as the recognition group. Once SO_2 and HClO were added, two significantly different emission peaks were observed, which achieved dual-color imaging of the two biomolecules. Using DNB, the authors realized simultaneous detection of endogenous and exogenous of SO_2 and HClO in HeLa cells under complex physiological conditions. Due to its outstanding two-photon advantages, DNB was also used to visualize SO_2 and HClO dynamic changes in zebrafish in depth. These novel probes inspire the exploration of new correlative mechanisms to sense RSS and ROS inbiological systems.

Wang's team synthesizes a TCAB based intramolecular cyclization for discriminative imaging of H_2O_2 and H_2S [66]. In this probe, coumarin- and piperazine-modified coumarin were used as dual-color fluorophores, and azide and boronate ester groups were used as common recognition sites for H_2S and H_2O_2. TCAB could identify H_2O_2 and H_2S with distinct fluorescence emission at 486 and 627 nm, respectively (Fig. 7). Moreover, the authors proved that TCAB had the capacity to monitor dynamic changes in both H_2O_2 and H_2S levels in HeLa cells and zebrafish. Based on the above mentioned FRET mechanism, the Bhuniya group also reports a fluorescent probe (PHS1) for imaging H_2O_2 and H_2S during the redox process [67]. PHS1 contained two fluorophores, coumarin and 1,8-naphthalene, and two recognition groups, azide and boronate ester. Compared with other active molecules (HClO, GSH, NO, Cys, etc.), PHS1 had excellent selectivity for H_2O_2 and H_2S. Using PHS1, elevated H_2O_2 and H_2S levels were observed in HeLa cells under phorbol myristate acetate (PMA) stimulation. The Yi group constructs a single-fluorescent probe 1 for synergistic detection of H_2S and H_2O_2 [68]. In the structure of probe 1, rhodamine and coumarin were selected as the double fluorophores, and the classical recognition groups of azide and boronate ester groups were grafted on the two fluorophores. When probe 1 reacted with H_2S, azide was reduced to an amino unit, and obvious fluorescence recovered owing to electron rearrangement of rhodamine. However, after the reaction with H_2O_2, the boronate ester group of probe 1 was degraded and produced a new coumarin with a strong "push-pull" system, resulting in strong fluorescence. When H_2O_2 and H_2S coexisted, an effective FRET effect occurred between rhodamine and coumarin, due to the admirable distance and overlapping spectra. Under excitation at 400 nm, the fluorescence intensity was enhanced at 520 nm. Moreover, probe 1 was successfully applied to simultaneous fluorescence imaging of endogenous H_2O_2 and H_2S in human embryonic kidney (HEK) 293 cells stimulated by PMA. Imaging experiment results confirmed that cysteine synthase played a key role in the production of H_2S.

Tang group has rationally designed a two-photon fluorescence probe (RPC-1) for the simultaneous discrimination of HClO and H_2S [69]. As shown in Fig. 8, RPC-1 used coumarin and rhodamine as double fluorophores, which were linked by piperazine. The azide and thiolactone groups were acted as specific recognition groups for H_2S and HClO, respectively. With the addition of H_2S, the strong fluorescence of coumarin recovered at 445 nm, since the azide group was rapidly reduced to the NH_2 moiety. Likewise, with the addition of HClO, thiolactone was oxidized to produce rhodamine with a strong fluorescence signal at 580 nm. When H_2S and HClO

Table 4 The classifications, chemical structures and applications of fluorescent probes for simultaneously detecting one ROS and one RSS

Classification	Chemical structure	Bioactive molecule	Wavelength/nm	Detection limit /(mol·L^{-1})	Application	Ref.
One ROS and one RSS	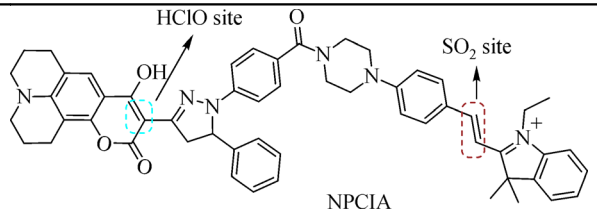	HClO and SO$_2$	ClO$^-$: 395/425, 544/585 HSO$_3^-$: 395/482	ClO$^-$: 1.66 × 10^{-8} HSO$_3^-$: 2.5 × 10^{-7}	In MCF-7, EC1, HeLa cells	[63]
	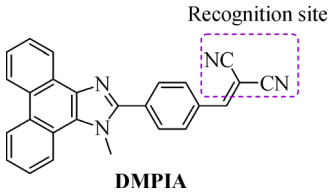	HClO and SO$_2$	ClO$^-$: 410/500, 410/625 SO$_2$: 330/410, 440/625	ClO$^-$: 1.25 × 10^{-8} SO$_2$: 3.5 × 10^{-9}	In HeLa cells and zebrafish	[64]
	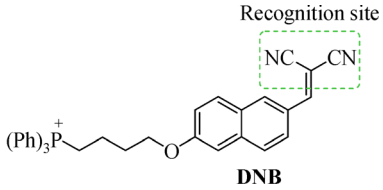	HClO and SO$_2$	ClO$^-$: 425/525, 425/600 HSO$_3^-$: 350/425, 460/600	ClO$^-$: 1.52 × 10^{-8} HSO$_3^-$: 8.0 × 10^{-9}	In HeLa cells and zebrafish	[65]
One RSS and one ROS	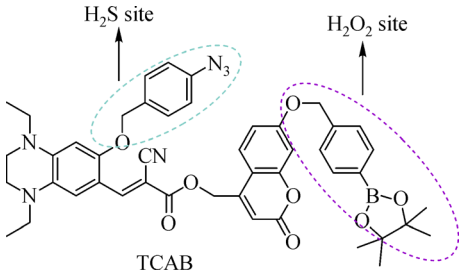	H$_2$S and H$_2$O$_2$	H$_2$S: 325/413, 475/627 H$_2$O$_2$: 325/486	H$_2$S: 5.8 × 10^{-8} H$_2$O$_2$: 4.4 × 10^{-8}	In HeLa cells and zebrafish	[66]
	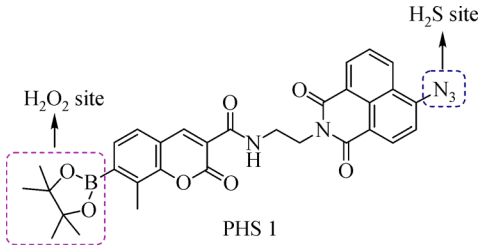	H$_2$S and H$_2$O$_2$	H$_2$S: 450/550 H$_2$O$_2$: 400/460	H$_2$S: 5.23 × 10^{-4} H$_2$O$_2$: 1.21 × 10^{-4}	In HeLa cells	[67]

(*Continued*)

Classification	Chemical structure	Bioactive molecule	Wavelength/nm	Detection limit /(mol·L^{-1})	Application	Ref.
	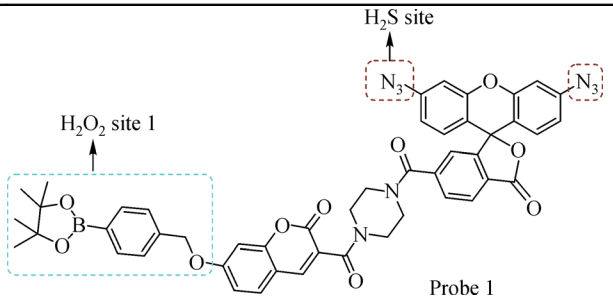	H_2S and H_2O_2	H_2S: 488/520 H_2O_2: 400/460	–	In HEK293 cells	[68]
One ROS and one RSS	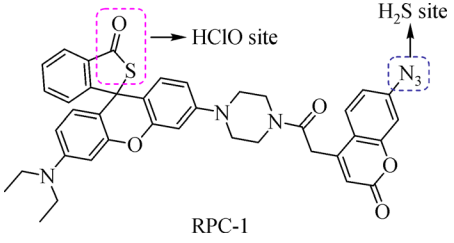	HClO and H_2S	ClO^-: 545/580 H_2S: 360/445	ClO^-: 1.98×10^{-8} H_2S: 1.92×10^{-7}	In RAW264.7 cells and mice	[69]
	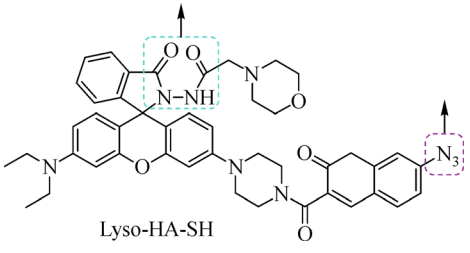	HClO and H_2S	ClO^-: 550/580 H_2S: 380/448	ClO^-: 7.3×10^{-8} H_2S: 3.5×10^{-7}	In HeLa cells	[70]
	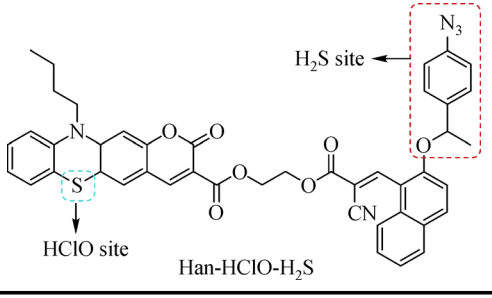	HClO and H_2S	ClO^-: 440/520, 440/640 H_2S: 400/450	ClO^-: 1.7×10^{-8} H_2S: 2.6×10^{-8}	In MCF-7 cells	[71]

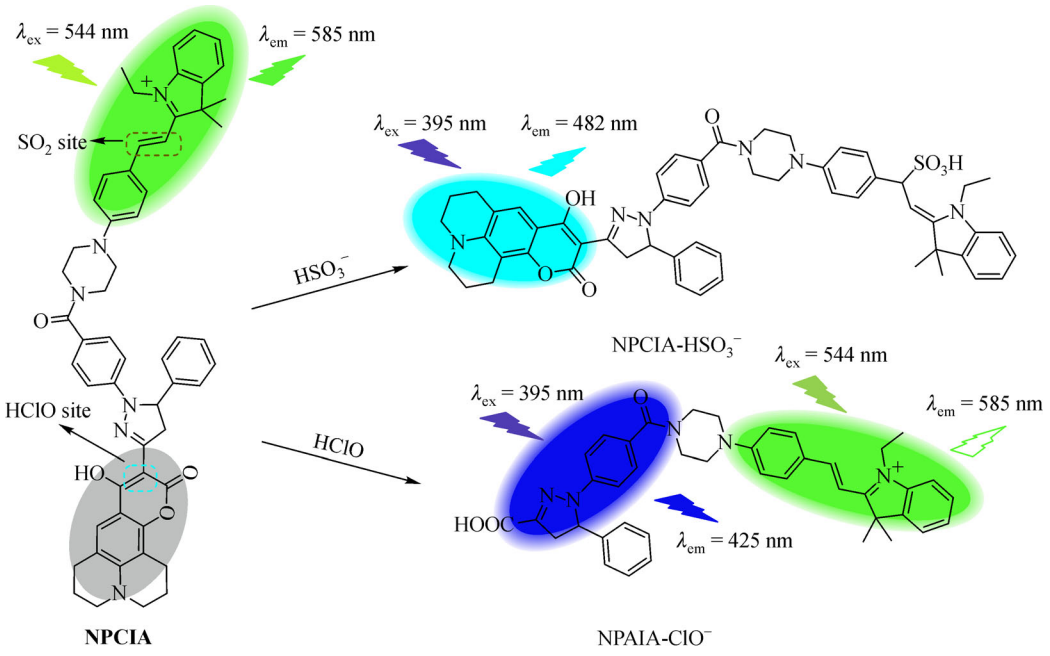

Fig. 6 Chemical structure and sensing mechanism proposed of NPCIA for the simultaneous detection of HClO and SO_2.

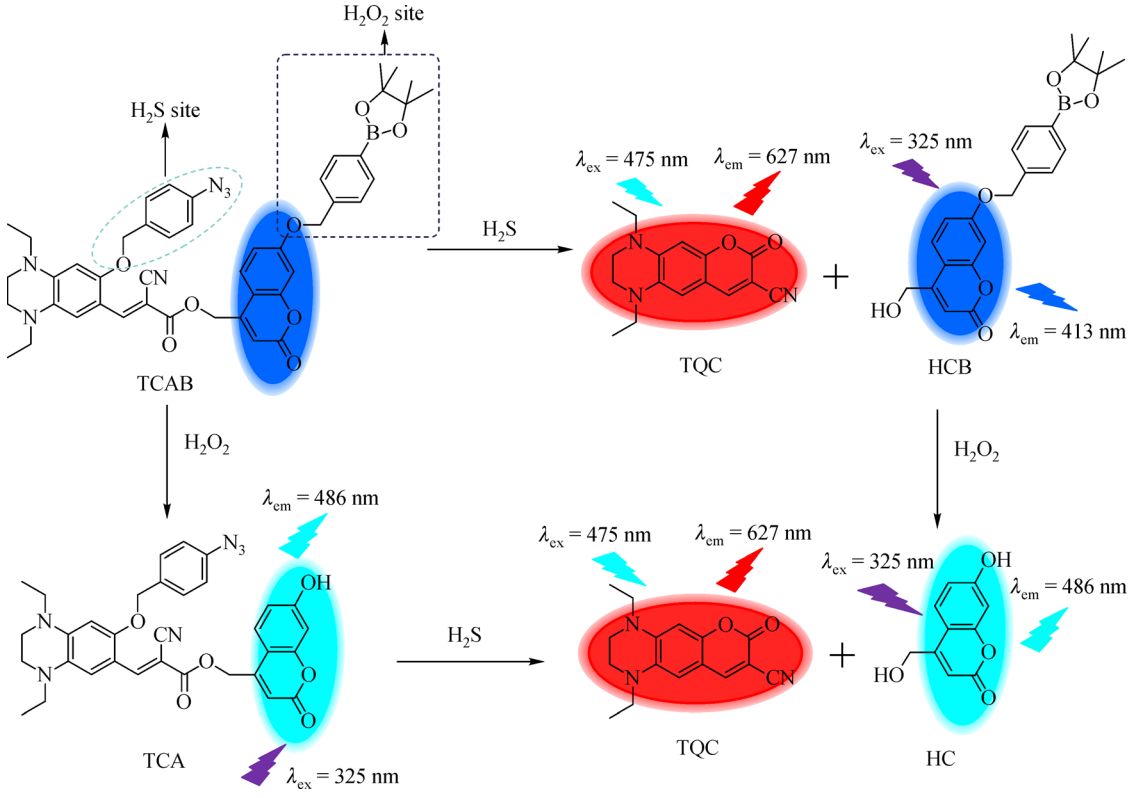

Fig. 7 The chemical structure of the TCAB and sensing mechanism proposed for detecting H_2O_2 and H_2S.

coexisted, RPC-1 could simultaneously distinguish H_2S from HClO with noninterfering emission spectra. With the excellent two-photon properties of RPC-1, it was visualized HClO and H_2S in living organism (Fig. 9). RPC-1 could be enabled to image endogenous H_2S and HClO in RAW264.7 cells after drug treatment (Fig. 9(A)). Moreover, *in vivo* experimental results illustrated that the levels of HClO and H_2S increased in drug-induced hepatotoxicity

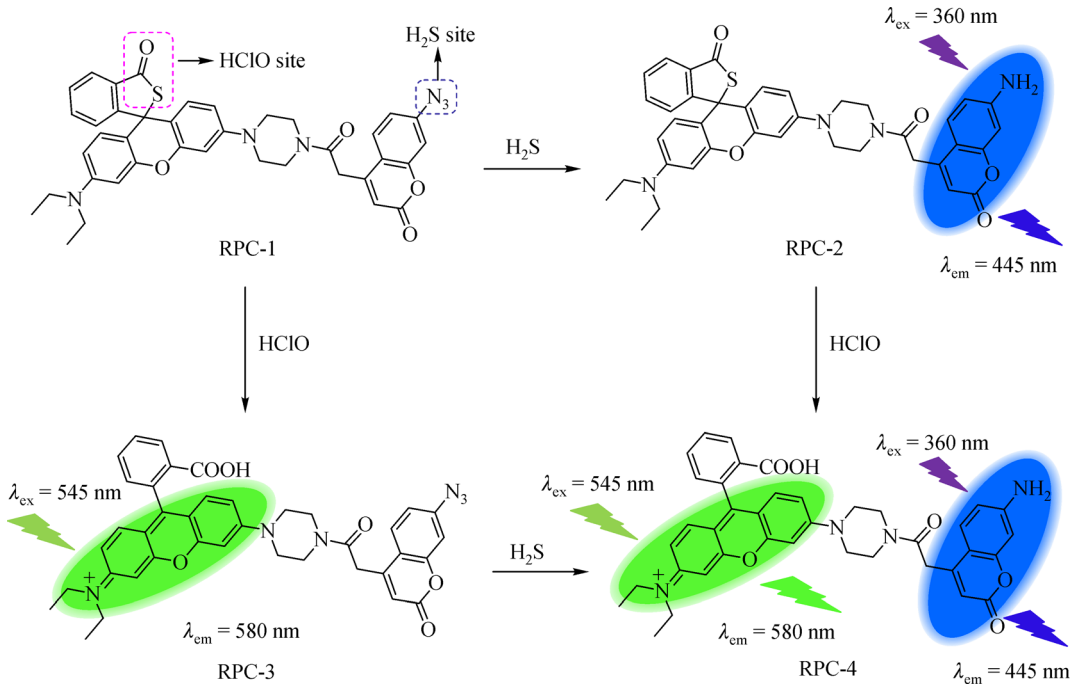

Fig. 8 The chemical structure and sensing mechanism proposed for RPC-1 for the discrimination of H_2S and HClO.

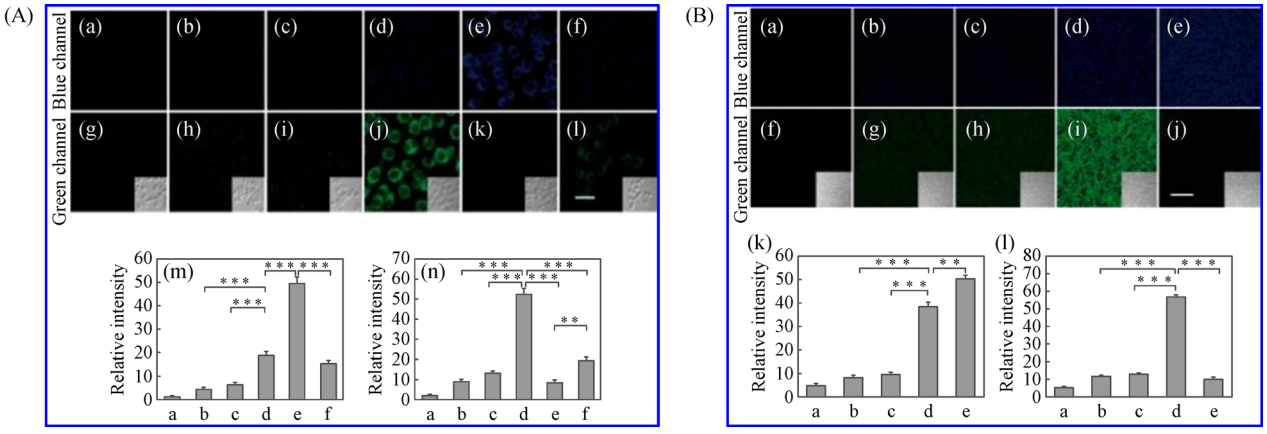

Fig. 9 (A) TPM images of RPC-1 endogenous H_2S and HClO in RAW264.7 cells after drug treatment; (B) TPM images of the RPC-1 of rat liver slices. Reprinted with permission from Ref. [69], copyright 2018 American Chemical Society.

(Fig. 9(B)). Subsequently, the Lin group reports a fluorescent probe, Lyso-HA-SH, that simultaneously responds to HClO and H_2S in lysosomes by a dual-responsive model [70]. In the probe, Lyso-HA-SH relied on rhodamine and coumarin as the double fluorophores, and morpholine as the targeting group of lysosomes. Moreover, both amide and azide units were arranged in the dyad. As expected, after the respective and successive reaction of HClO and H_2S, Lyso-HA-SH exhibited distinct fluorescence emission signal patterns. Lyso-HA-SH was successfully used for imaging of exogenous HClO and H_2S in lysosomes. Interestingly, Lyso-HA-SH only detected an increase in H_2S levels in HeLa cells, but not HClO under LPS and PMA stimulation. The Song group synthesizes a new ratiometric chemosensor (Han-HClO-H_2S) for the simultaneous detection of HClO and H_2S [71]. Han-HClO-H_2S had two reaction sites, namely, the phenothiazine portion and azide group. The phenolthiazine portion was oxidized by HClO, resulting in a fluorescence emission peak from red (640 nm) to green (520 nm) for ratiometric imaging. The azide group reacted with H_2S to generate coumarin with blue fluorescence (450 nm), while phenothiazine with red fluorescence (640 nm) was retained. The cell imaging results showed that ratiometric imaging of H_2S and HClO was realized in Michigan Cancer Foundation-7 (MCF-7) cells. These works provide

three powerful imaging tools for studying the synergistic interaction between H_2S and HClO in cells and organelles, as well as in deep tissues *in vivo*.

2.5 Simultaneous imaging of one reactive nitrogen species (RNS) and one RSS

RNS are another important group of oxidative species in organisms, mainly including nitric oxide (NO) and peroxynitrite [72,73]. RNS also play pivotal roles in signal transduction and cell function [74]. RNS show strong oxidation ability, causing irreversible damage to lipids, proteins and DNA, and ultimately leading to a variety of diseases [75]. To better illustrate the relationships between RNS and RSS during the initiation and development of various diseases, researchers have developed fluorescent probes to simultaneously detect RNS and RSS (Table 5).

The Wu group prepares a FRET-based fluorescent probe (Naph-RhB) that permits the simultaneous detection of exogenous H_2S and NO in living L929 cells [76]. For Naph-RhB, azide-modified naphthalimide and *o*-phenylenediamine-connected rhodamine were attached via piperazine, which guaranteed an efficient FRET process between naphthalimide and rhodamine (Fig. 10). Initially, Naph-RhB itself exhibited negligible fluorescence, due to electron withdrawal of azide and spirocyclic lactone forms. While azide was reduced to amino group by H_2S, the fluorescence of naphthalene was enhanced. In the presence of NO, the spirocyclic lactone was broken to form rhodamine with an open ring structure, and fluorescence was emitted. Then, the FRET process occurred from the naphthalene to rhodamine moiety, since there was obvious spectral overlap between the two fluorophores. Furthermore, Naph-RhB showed eminent advantages, such as high selectivity, quick response and high sensitivity. Based on these results, Naph-RhB will be a favorable chemical tool to investigate the interplay of H_2S and NO in complex biological environments.

The Yang group reports a series of dual-response fluorescent probes for the simultaneous detection of NO and GSH based on BODIPY dye [77]. 4-Amino-3-(methylamino)-phenol was introduced as the recognition group for NO and GSH. Among probes, probe 1 showed weak fluorescence due to the PET mechanism. As expected, the reaction with NO triggered remarkable fluorescence of probe 1 at 528 nm, because the diamine moiety was converted to a triazole group. Additionally, phenol was replaced by GSH through a nucleophilic aromatic substitution reaction, causing the fluorescence emission redshift (558 nm). With high selectivity and a rapid response, probe 1 successfully visualized changes in the levels of exogenous and endogenous NO and GSH in macrophages. By further application of probe 1, the cross-talk between NO and GSH was revealed under various stimuli, such as interferon, LPS and L-arginine.

2.6 Simultaneous imaging of two other biomolecules

Understanding the cross-talk of other reactive molecules in complex systems is also imperative, since they have interlinked functions in prevalent disorders, including inflammation and liver diseases [78,79]. Some selective and sensitive fluorescent probes have been developed for the simultaneous detection of two other biomolecules (Table 6). For example, the Lin group constructs a dual-response fluorescent probe, FP-H_2O_2-NO, which is capable of endogenously detecting produced H_2O_2 and NO [80]. In this structure, the H_2O_2-responsive boronate moiety was anchored to the coumarin dye, while NO-responsive *o*-phenylenediamine was connected to rhodamine (Fig. 11). After the reaction of FP-H_2O_2-NO with H_2O_2, the boronate moiety was degraded to generate coumarin with a strong "push-pull" structure, leading to enhanced fluorescence centered at 460 nm with excitation at 400 nm. Under NO treatment, the amide bond was destroyed, and an open ring system of rhodamine was formed. Under excitation at 550 nm, strong fluorescence at 580 nm was emitted. When H_2O_2 and NO coexist under complex conditions, the emission spectra of the donor effectively overlap with the absorption spectra of the acceptor, resulting in the FRET effect. Therefore, regardless of whether excitation occurred at 400 or 550 nm, strong fluorescence at 580 nm was observed. By using fluorescence confocal microscopy, the increase of H_2O_2 and NO levels were simultaneously monitored in HeLa and RAW264.7 cells in the absence or presence of stimuli (Fig. 12).

The Tian group has developed a two-photon excited fluorescence lifetime probe (TFP) that can detect changes in mitochondrial H_2O_2 and adenosine triphosphate (ATP) simultaneously, selectively and in real-time [81]. In the design, the fluorescence of fluorophores was effectively quenched by the phenylborate ester and spirolactam ring rhodamine (Fig. 13). Moreover, pyridine cation could contribute TFP to accumulate in mitochondria. Upon the addition of H_2O_2, a strong fluorescence signal was observed, owing to cleavage of the benzene boronic acid pinacol ester bond. Multiple amino groups of TFP could form hydrogen bonds with ATP, causing fluorescence enhancement. Importantly, these two emission peaks did not overlap with each other in the presence of H_2O_2 and ATP. Hence, TFP had the ability to simultaneously detect H_2O_2 and ATP. Subsequently, TFP was applied to detect intracellular changes in H_2O_2 and ATP contents in mitochondria under different stimulation conditions by fluorescence lifetime imaging. Furthermore, due to the outstanding performance of TFP, it was successfully used to analyze the changes in H_2O_2 and ATP levels in zebrafish under normal and hypoxic conditions.

The Zhang group has synthesized a single fluorescent probe, N_3-CR-PO_4, that can simultaneously distinguish H_2S from alkaline phosphatase (ALP) using two well-

Table 5 The classifications, chemical structures and applications of fluorescent probes for simultaneously detecting one RSS and one RNS

Classification	Chemical structure	Bioactive molecule	Wavelength/nm	Detection limit/(mol·L^{-1})	Application	Ref.
One RSS and One RNS	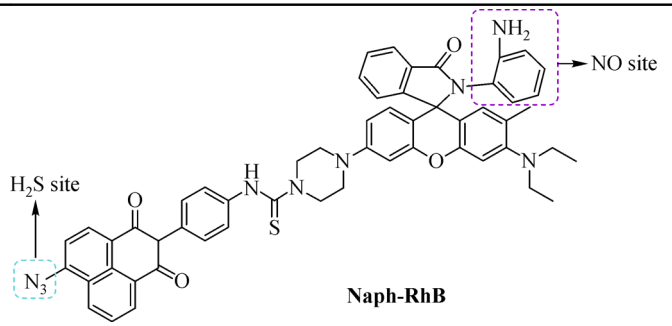	NO and H_2S	NO: 550/570 H_2S: 425/539	–	In L929 cells	[76]
	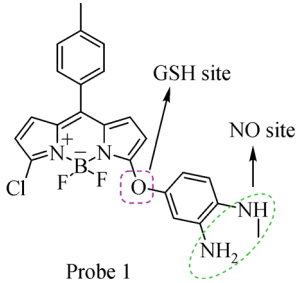	NO and GSH	NO: 505/528 GSH: 538/558	NO: 3.1×10^{-8} GSH: 5.6×10^{-8}	In macrophages	[77]

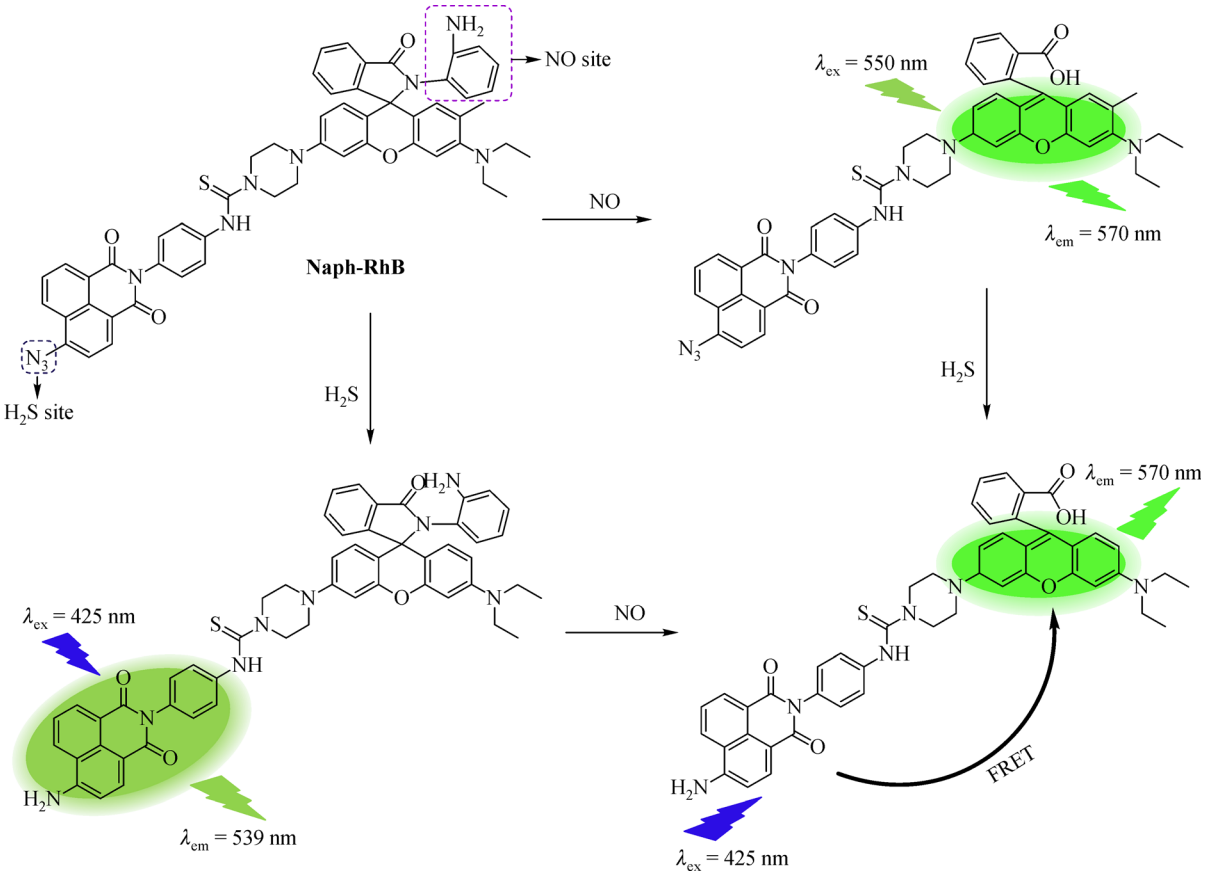

Fig. 10 The chemical structure of Naph-RhB and the sensing mechanism proposed for monitoring NO and H_2S.

separated fluorescence signals [82]. N_3-CR-PO_4 contained two fluorophores, coumarin and fluorescein, that were connected through a rigid piperazine. They chose azide and phosphate groups as recognition sites for H_2S and ALP, respectively. With the addition of H_2S, the azide group was reduced to NH_2, and a coumarin structure with a strong "push-pull" system was formed, emitting strong fluorescence at 445 nm. With the addition of ALP, phosphate ester bonds were hydrolyzed, leading to dramatic increases in absorption and fluorescence signals (545 nm). However, the FRET process would occur between coumarin and fluorescein, since the fluorescence spectra of coumarin efficiently coincided with the absorption spectra of fluorescein. The imaging experiments confirmed that the decrease in H_2S levels might lead to the inactivation of ALP in living cells.

The Ma group reports a dual-responsive fluorescent probe for the simultaneous and selective detection of nitroreductase (NRT) and ATP [83]. To obtain this probe, a rhodamine and 1,8-naphthalene were used as double fluorophores. And nitro and diethylenetriamine groups were served as recognition sites for NTR and ATP, respectively. When the probe reacted with NTR, the nitro group was reduced to amino group, leading to a bright fluorescence signal of 1,8-naphthalimide (520 nm). In the presence of ATP, the amide group of the probe was broken, and a ring-opening rhodamine was formed, eventually emitting strong fluorescence (580 nm). Interestingly, the FRET process appeared between naphthalimide and rhodamine under simultaneous treatment with NRT and ATP. Notably, this probe was the first to reveal the negative interrelation between intracellular NTR and ATP under hypoxic conditions, which confirmed ATP as a hypoxia-sensitive species. Moreover, a dual-color small molecule fluorescent probe has been developed for monitoring the activity of glycosidase and phosphodiesterase 1 (PDE) with various optical imaging modes [84]. In the initial probe design, the probe contained two fluorochromes (mesotetraphenylporphyrin and 7-hydroxycoumarin) with distinct signal readouts, and two recognition sites specifically reacting with β-D-gluconeinase (GCD) and PDE, respectively. Based on the PET mechanism, the probe showed weak fluorescence. However, the probe possessed different fluorescence signal output after it reacted with two enzymes. Confocal fluorescence imaging showed that the activity of GCD and PDE was significantly increased in Huh7 cells.

The Jiang group has synthesized a fluorescent probe 1 based on BODIPY for the simultaneous detection of fluoride (F^-) and H_2S, which used trihexylsilylacetylene

Table 6 The classifications, chemical structures and applications of fluorescent probes for simultaneously detecting two other biomolecules

Classification	Chemical structure	Bioactive molecule	Wavelength/nm	Detection limit	Application	Ref.
One ROS/one RNS	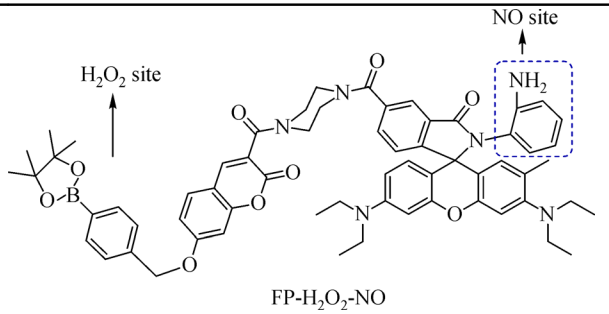	H_2O_2 and NO	H_2O_2: 400/460 NO: 550/580	–	In HeLa and RAW264.7 cells	[80]
One ROS/one macromolecule	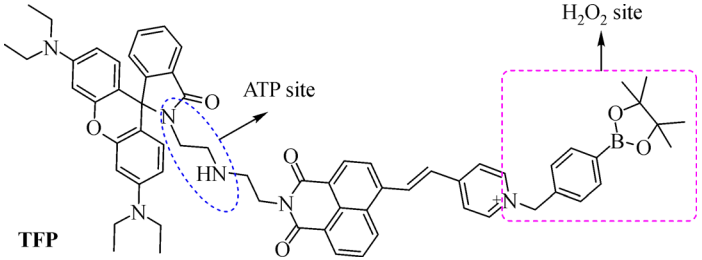	H_2O_2 and ATP	H_2O_2: 710/470 ATP: 710/590		In living cells and zebrafish	[81]
One RSS/one macromolecule	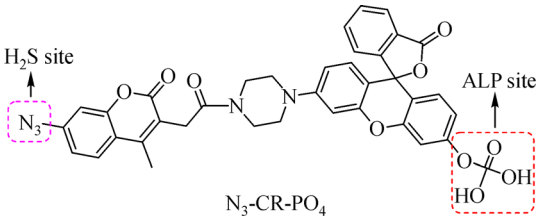	H_2S and ALP	H_2S: 360/445 ALP: 510/545		In HeLa cells	[82]

(*Continued*)

Classification	Chemical structure	Bioactive molecule	Wavelength/nm	Detection limit	Application	Ref.
Two macromolecules	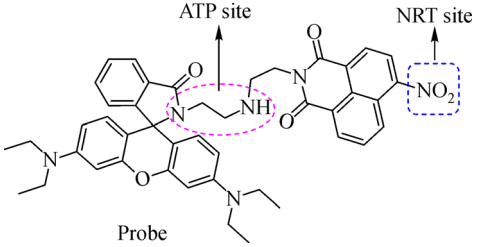	ATP and NRT	ATP: 540/580 NRT: 420/520	ATP: 0.05 mmol·L^{-1} NRT: 0.12 μg·mL^{-1}	In HeLa cells	[83]
	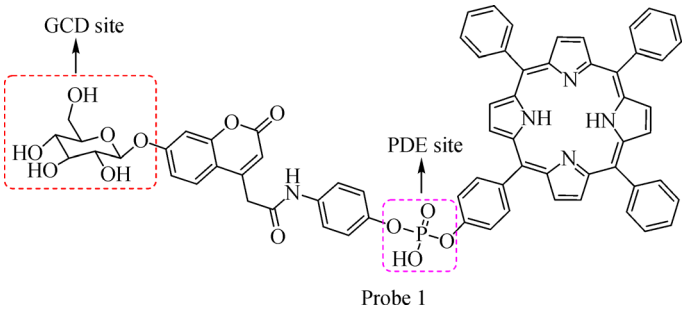	GCD and PDE	GCD: 340/460 PDE: 340/656	GCD: 1 U	In Huh7 cells	[84]
One RSS/F$^-$	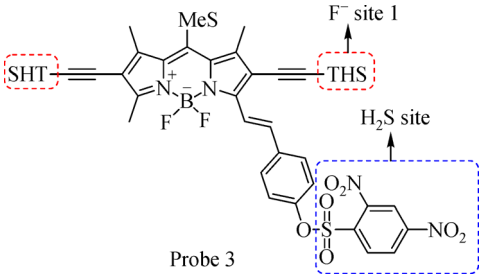	F$^-$ and H$_2$S	F$^-$: 365/553 HS$^-$: 550/633	F$^-$: 1.45 × 10^{-8} HS$^-$: 5.73 × 10^{-8}	In HeLa cells	[85]

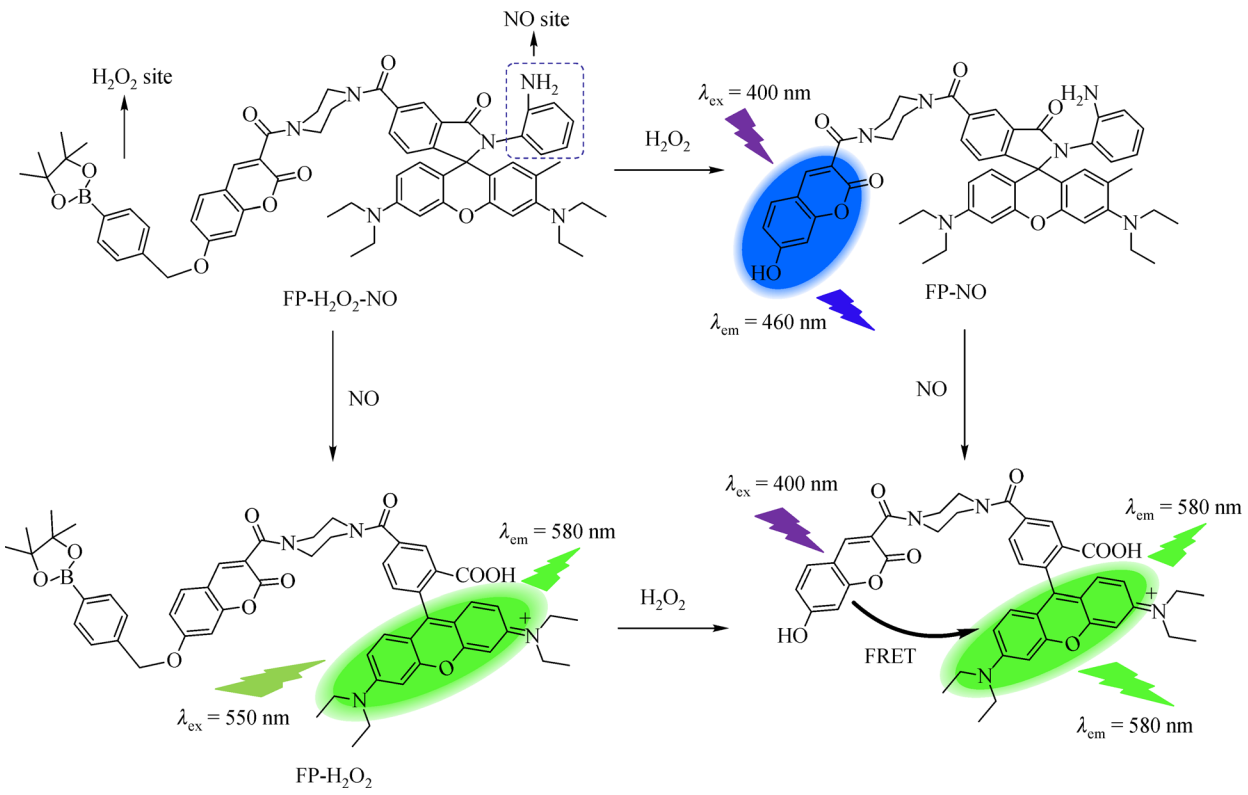

Fig. 11 Chemical structure and proposed detection mechanism of FP-H_2O_2-NO for discrimination of H_2O_2 and ATP.

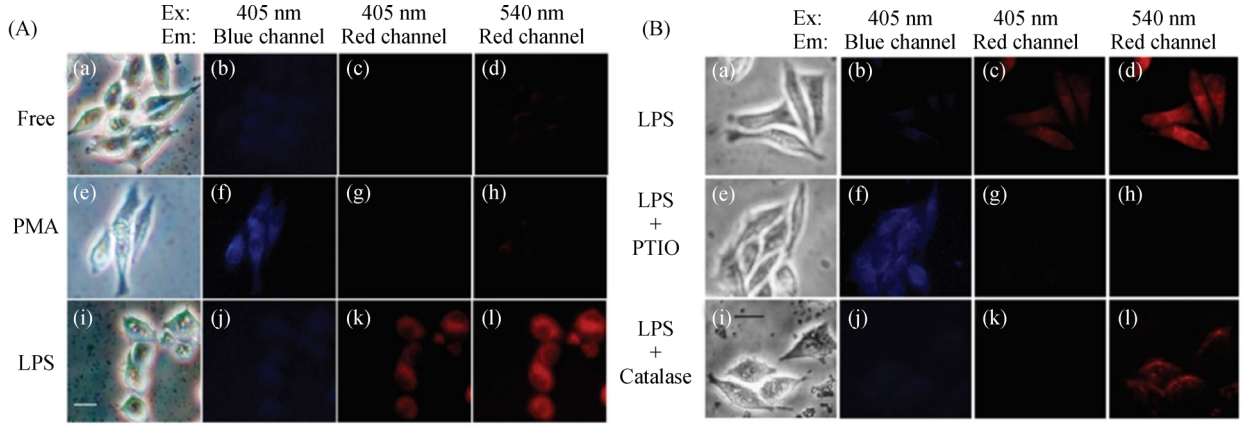

Fig. 12 (A) Fluorescence imaging of FP-H_2O_2-NO in living RAW264.7 cells in the absence or presence of stimuli; (B) Fluorescence imaging of FP-H_2O_2-NO in living RAW264.7 cells in the absence or presence of stimuli and scavengers. Reprinted with permission from Ref. [80], copyright 2011 American Chemical Society.

(THS) and 2,4-nitrobenzenesulfonyl (DNBS) as the two recognition units of F^- and H_2S, respectively [85]. With the increase of F^- level, the THS was degraded, and fluorescence at 553 nm was emitted. With the increase of H_2S, the DNBS group was also degraded, and fluorescence at 633 nm was emitted. The virtues of high selectivity and sensitivity helped probe 1 successfully visualize H_2S in live HeLa cells. Therefore, these works may provide novel strategies for exploring and discovering novel functions and roles of reactive molecule-related diseases.

3 Discussion

In this review, we summarize the structures, recognition mechanisms and imaging applications of reported small molecule fluorescent probes for the simultaneous detection of two bioactive molecules in living cells and *in vivo*. Despite substantial advances in this field, the development and applicability of dual-response probes are still limited to some extent. The main reasons are as follows. One of the greatest challenges is that fluorescence emission wave-

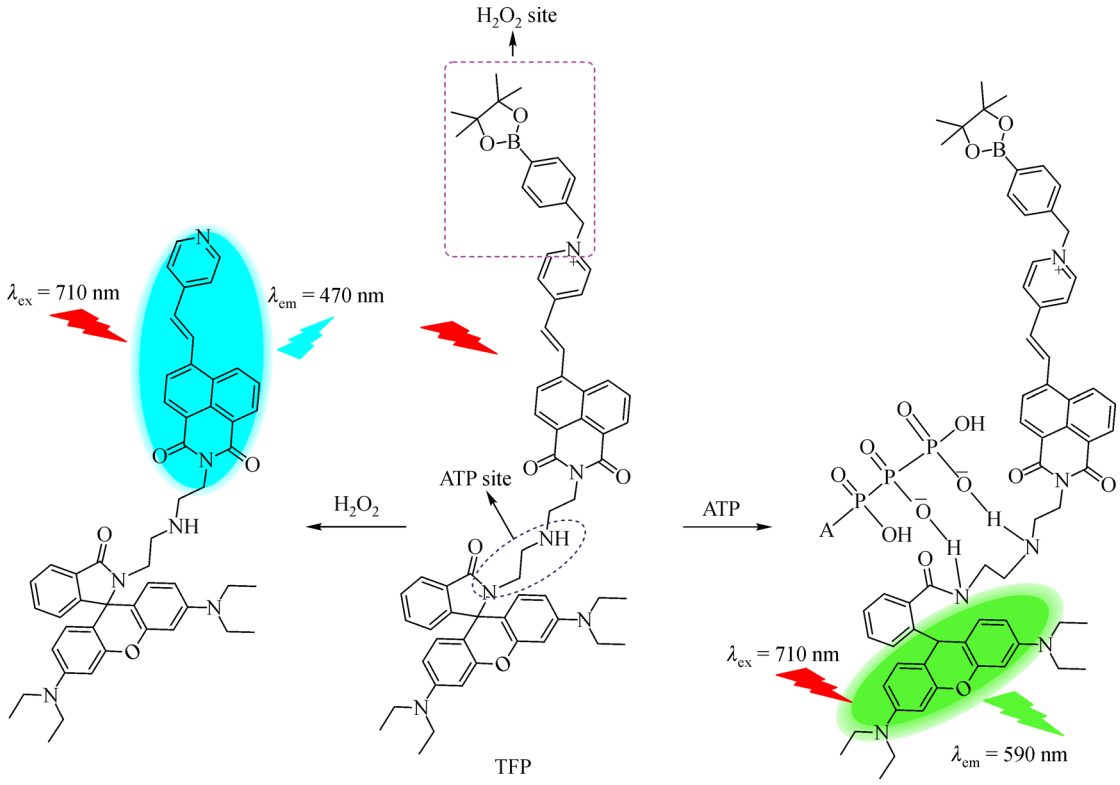

Fig. 13 Chemical structure and proposed detection mechanism of TFP for discrimination of H_2O_2 and ATP.

lengths between the fluorophores in probes and corresponding products are so similar that they cause fluorescence spectra crosstalk, and eventually result in indistinguishable detection of two species, such as BDNOL, 2-QMP, probe 2, 3o and probe 1 (Jiang). Therefore, we preferred to design some single fluorescence probes that yielded two unique and differentiable fluorescence signals in the presence of both analytes. A notable example is the POP, which possesses a single fluorophore and a recognition group and emits two fluorescence signals at 545 and 620 nm when Cys and GSH coexist.

Second, to further study the concentration variation of the two analytes under physiological conditions, ratiometric systems are selected as an excellent approach. At present, there are two ways of ratio-imaging to not only exclude the influence of the probe concentration, but also detect the targets quantitatively. In one approach, probe itself has fluorescence, which emitted different fluorescence signals after it reacts with two analytes, such as TCAB, CSU1, Han-HClO-H_2S, MPIBA and DNB. The other approach is a hot topic in the fluorescence imaging field. The ratiometric response of the probe can also be monitored by fluorescence lifetime microscopy, since the fluorescence lifetime is independent of the probe concentration. To date, some lifetime-based probes have been reported for detecting single analyte. However, the only dual-responsive fluorescence lifetime-based two-photon probe reported to date is TFP, which can simultaneously achieve real-time and quantitative determination of the concentration changes of mitochondrial H_2O_2 and ATP by fluorescence lifetime microscopy. Therefore, fluorescence lifetime method is likely to be a fruitful field of probe design in the future.

Last does not mean unimportant, these above review show that most of these probes, such as NIR-Cys, Z2, MC-Sn, RPC-1, Lyso-HA-HS, and DNB, can be used to observe the dynamic changes and distributions of two reactive molecules in deep tissue owing to their excellent performance in penetration ability. However, compared with two-photon or near-infrared fluorescent probes, the *in vivo* application of one-photon probes is limited by their short excitation wavelengths. Hence, there is an urgent need to develop two-photon or near-infrared fluorescent probes to study the synergistic molecular mechanisms of bioactive molecules *in vivo*.

4 Summary and perspective

Interrelationships and synergistic regulations of two bioactive molecules play crucial roles in cells and *in vivo*. Dual-detection fluorescence probes for bioactive species to uncover this interplay and regulations have attracted increasing attention in recent years. In this review, we concentrate on the performances and characteristics of existing single-structure and dual-responsive fluorescence

probes, such as nondestructive, real time, in situ and rapid quantitative detection. Moreover, these probes can be effective imaging tools to visualize the dynamic interplay between two reactive molecules under some pathological conditions.

Although a class of dual-response probes has been developed and applied for monitoring two bioactive molecules in biological systems, further study of new synergistic interactions and signaling pathways is needed. Hence, in the next few years, the development of dual-responsive small molecular fluorescent probes for biomolecules should consider the following approaches: (a) Multi-modal imaging probes should be designed to precisely track the variations of reactive molecules *in vivo*, such as fluorescence and photoacoustic imaging; (b) ratiometric fluorescence probes need to be designed for quantitative analysis of metal ions, free radicals, anions and enzymes in biological systems; (c) organelle-targeting probes should be developed for the early diagnosis and treatment of various related diseases; (d) two-photon and NIR probes will be integrated, especially probes with absorption wavelengths in the NIR-II region of NIR probes.

In conclusion, the development of novel fluorescence probes for the simultaneous identification of two reactive molecules is still a hot topic in the field of fluorescence imaging. Achieving this goal will help to clarify the complex interactions and synergistic regulatory effects of multiple biomolecules, and it is essential for understanding the underlying molecular mechanisms of related diseases *in vivo*.

Acknowledgements This work was supported by the National Natural Science Foundation of China (Grant Nos. 91753111, 22074083 and 21927811), the Key Research and Development Program of Shandong Province (Grant No. 2018YFJH0502), and the National Major Scientific and Technological Special Project for Significant New Drugs Development (Grant No. 2017ZX09301030004).

References

1. Sies H, Jones D P. Reactive oxygen species (ROS) as pleiotropic physiological signaling agents. Nature Reviews. Molecular Cell Biology, 2020, 21(7): 363–383
2. Sies H, Berndt C, Jones D P. Oxidative stress. Annual Review of Biochemistry, 2017, 86(1): 715–748
3. Wu L L, Huang C, Emery B P, Sedgwick A C, Bull S D, He X P, Tian H, Yoon J Y, Sessler J L, James T D. Forster resonance energy transfer (FRET)-based small-molecule sensors and imaging agents. Chemical Society Reviews, 2020, 49(15): 5110–5139
4. Chen W, Pacheco A, Takano Y K, Day J J, Hanaoka K, Xian M. A single fluorescent probe to visualize hydrogen sulfide and hydrogen polysulfides with different fluorescence signals. Angewandte Chemie International Edition, 2016, 55(34): 9993–9996
5. Chen X Q, Wang F, Hyun J Y, Wei T W, Qiang J, Ren X T, Shin I J, Yoon J Y. Recent progress in the development of fluorescent, luminescent and colorimetric probes for detection of reactive oxygen and nitrogen species. Chemical Society Reviews, 2016, 45 (10): 2976–3016
6. Xu Z, Xu L. Fluorescent probes for the selective detection of chemical species inside mitochondria. Chemical Communications, 2016, 52(6): 1094–1119
7. Mao Z Q, Ye M T, Hu W, Ye X X, Wang Y Y, Zhang H J, Li C Y, Liu Z H. Design of a ratiometric two-photon probe for imaging of hypochlorous acid (HClO) in wounded tissues. Chemical Science (Cambridge), 2018, 9(28): 6035–6040
8. Li X H, Gao X H, Shi W, Ma H M. Design strategies for water-soluble small molecular chromogenic and fluorogenic probes. Chemical Reviews, 2014, 114(1): 590–659
9. Harris I S, DeNicola G D. The complex interplay between antioxidants and ROS in cancer. Trends in Cell Biology, 2020, 30 (6): 440–451
10. Jiao X Y, Li Y, Niu J Y, Xie X L, Wang X, Tang B. Small-molecule fluorescent probes for imaging and detection of reactive oxygen, nitrogen, and sulfur species in biological systems. Analytical Chemistry, 2018, 90(1): 533–555
11. Wu D, Sedgwick A C, Gunnlaugsson T, Akkaya E U, Yoon J Y, Jame T D. Fluorescent chemosensors: the past, presen and future. Chemical Society Reviews, 2017, 46(23): 7105–7123
12. Gao P, Pan W, Li N, Tang B. Fluorescent probes for organelle-targeted bioactive species imaging. Chemical Science (Cambridge), 2019, 10(24): 6035–6071
13. Ueno T, Nagano T. Fluorescence probes for sensing and imaging. Nature Methods, 2011, 8(8): 642–645
14. Zhu J L, Xu Z, Yang Y Y, Xu L. Small-molecule fluorescent probes for specific detection and imaging of chemical species inside lysosomes. Chemical Communications, 2019, 55(47): 6629–6671
15. Yuan L, Lin W Y, Zhang K B, Zhu S S. FRET-based small-molecule fluorescent probes: rational design and bioimaging applications. Accounts of Chemical Research, 2013, 46(7): 1462–1473
16. He L W, Dong B L, Liu Y, Lin W Y. Fluorescent chemosensors manipulated by dual/triple interplaying sensing mechanisms. Chemical Society Reviews, 2016, 45(23): 6449–6461
17. Crichton R R, Pierre J L. Old iron, young copper: from Mars to Venus. Biometals, 2011, 14(2): 99–112
18. Wang X, Li P, Zhang W, Tang B. Recent advances in fluorescence imaging of bioactive molecules in neurons and *in vivo*. Chinese Journal of Analytical Chemistry, 2019, 47(10): 1537–1548
19. Lee M H, Kim J S, Sessler J L. Small molecule-based ratiometric fluorescence probes for cations, anions, and biomolecules. Chemical Society Reviews, 2015, 44(13): 4185–4191
20. Miller L M, Wang Q, Telivala T P, Smith R J, Lanzirotti A, Miklossy J. Synchrotron-based infrared and X-ray imaging shows focalized accumulation of Cu and Zn co-localized with β-amyloid deposits in Alzheimer's disease. Journal of Structural Biology, 2006, 155(1): 30–37
21. Nakao N, Frodl E V, Widner H, Carlson E, Eggerding F A, Epstein C J, Brundin P. Overexpressing Cu/Zn superoxide dismutase enhances survival of transplanted neurons in a rat model of Parkinson's disease. Nature Medicine, 1995, 1(3): 226–231
22. Hou L J, Feng J, Wang Y B, Dong C A, Shuang S M, Wang Y.

Single fluorescein-based probe for selective colorimetric and fluorometric dual sensing of Al^{3+} and Cu^{2+}. Sensors and Actuators. B, Chemical, 2017, 247: 451–460
23. Roy A, Shee U, Mukherjee A, Mandal S K, Roy P. Rhodamine-based dual chemosensor for Al^{3+} and Zn^{2+} ions with distinctly separated excitation and emission wavelengths. ACS Omega, 2019, 4(4): 6864–6875
24. Hazra A, Roy A, Mukherjee A, Maiti G P, Roy P. Remarkable difference in Al^{3+} and Zn^{2+} sensing properties of quinoline based isomers. Dalton Transactions (Cambridge, England), 2018, 47(39): 13972–13989
25. Sun W, Li M, Fan J L, Peng X J. Activity-based sensing and theranostic probes based on photoinduced electron transfer. Accounts of Chemical Research, 2019, 52(10): 2818–2831
26. Zhao G, Wei G, Yan Z Q, Guo B Y, Guang S Y, Wu R L, Xu H Y. A multiple fluorescein-based turn-on fluorophore (FHCS) identified for simultaneous determination and living imaging of toxic Al^{3+} and Zn^{2+} by improved stokes shift. Analytica Chimica Acta, 2020, 1095: 185–196
27. Liu H Y, Liu T Q, Li J, Zhang Y M, Li J H, Song J, Qu J L, Wong W Y. A simple Schiff base as dual-responsive fluorescent sensor for bioimaging recognition of Zn^{2+} and Al^{3+} in living cells. Journal of Materials Chemistry. B, Materials for Biology and Medicine, 2018, 6(34): 5435–5442
28. Erdemir S, Yuksekogu M, Karakurt S, Kocyigit O. Dual-channel fluorescent probe based on bisphenol A-rhodamine for Zn^{2+} and Hg^{2+} through different signaling and its bioimaging studies. Sensors and Actuators B Chemiscal, 2017, 241: 230–238
29. Wu L L, Sedgwick A C, Sun X L, Bull S D, He X P, James T D. Reaction-based fluorescent probes for the detection and imaging of reactive oxygen, nitrogen, and sulfur species. Accounts of Chemical Research, 2019, 52(9): 2582–2597
30. Zhao Y, Zheng B Z, Du J, Xiao D, Yang L. A fluorescent "turn-on" probe for the dual-channel detection of Hg(II) and Mg(II) and its application of imaging in living cells. Talanta, 2011, 85(4): 2194–2201
31. Andina D, Leroux J C, Luciani P. Ratiometric fluorescent probes for the detection of reactive oxygen species. Chemistry (Weinheim an der Bergstrasse, Germany), 2017, 23(55): 13547–13573
32. Schoenfeld J D, Sibenaller Z A, Mapuskar K A, Wagner B A, Cramer-Morales K L, Furqan M, Sandhu S, Carlisle T L, Smith M C, Abu Hejleh T, et al. $O_2^{\cdot-}$ and H_2O_2-mediated disruption of Fe metabolism causes the differential susceptibility of NSCLC and GBM cancer cells to pharmacological ascorbate. Cancer Cell, 2017, 31(4): 487–500
33. Lou Z R, Li P, Han K L. Redox-responsive fluorescent probes with different design strategies. Accounts of Chemical Research, 2015, 48(5): 1358–1368
34. Hassannia B, Vandenabeele P, Vanden Berghe T. Targeting ferroptosis to iron out cancer. Cancer Cell, 2019, 35(6): 830–849
35. Chouchani E T, Pell V R, Gaude E, Aksentijević D, Sundier S Y, Robb E L, Logan A, Nadtochiy S M, Ord E N J, Smith A C, et al. Ischaemic accumulation of succinate controls reperfusion injury through mitochondrial ROS. Nature, 2014, 515(7527): 431–435
36. He F, Zuo L. Redox roles of reactive oxygen species in cardiovascular disease. International Journal of Molecular Sciences, 2015, 16(11): 27770–27780
37. Zhang R, Zhao J, Han G, Liu Z, Liu C, Zhang C, Liu B, Jiang C, Liu R, Zhao T, Han M Y, Zhang Z. Real-time discrimination and versatile profiling of spontaneous ROS in living organisms with a single fluorescent probe. Journal of the American Chemical Society, 2016, 138(11): 3769–3778
38. Du Y C, Wang B W, Jin D, Li M R, Li Y, Yan X L, Zhou X Q, Chen L G. Dual-site fluorescent probe for multi-response detection of ClO^- and H_2O_2 and bio-imaging. Analytica Chimica Acta, 2020, 1103: 174–182
39. Han J L, Liu X J, Xiong H Q, Wang J P, Wang B H, Song X Z, Wang W. Investigation of the relationship between H_2O_2 and HClO in living cells by a bifunctional, dual-ratiometric responsive fluorescent probe. Analytical Chemistry, 2020, 92(7): 5134–5142
40. Park S H, Kwon N, Lee J H, Yoon J Y, Shin I. Synthetic ratiometric fluorescent probes for detection of ions. Chemical Society Reviews, 2020, 49(1): 143–179
41. Long L L, Han Y Y, Liu W G, Chen Q, Yin D D, Li L L, Yuan F, Han Z X, Gong A H, Wang K. Simultaneous discrimination of hypochlorite and single oxygen during sepsis by a dual-functional fluorescent probe. Analytical Chemistry, 2020, 92(8): 6072–6080
42. Yue Y K, Huo F J, Cheng F Q, Zhu X J, Mafireyi T, Strongin R M, Yin C X. Functional synthetic probes for selective targeting and multi-analyte detection and imaging. Chemical Society Reviews, 2019, 48(15): 4155–4177
43. Chen X Q, Zhou Y, Peng X J, Yoon J Y. Fluorescent and colorimetric probes for detection of thiols. Chemical Society Reviews, 2010, 39(6): 2120–2135
44. Lin V S, Chen W, Xian M, Chang C J. Chemical probes for molecular imaging and detection of hydrogen sulfide and reactive sulfur species in biological systems. Chemical Society Reviews, 2015, 44(14): 4596–4618
45. Yu F B, Han X Y, Che L X. Fluorescent probes for hydrogen sulfide detection and bioimaging. Chemical Communications, 2014, 50 (82): 12234–12249
46. Zhou Y Q, Li P, Fan N N, Wang X, Liu X N, Wu L J, Zhang W, Zhang W, Ma C L, Tang B. *In situ* visualization of peroxisomal peroxynitrite in the livers of mice with acute liver injury induced by carbon tetrachloride using a new two-photon fluorescent probe. Chemical Communications, 2019, 55(47): 6767–6770
47. Zhang H X, Liu J, Hu B, Wang L F, Yang Z, Han X, Wang J J, Bai W, Guo W. Dual-channel fluorescence diagnosis of cancer cells/tissues assisted by OATP transporters and cysteine/glutathione. Chemical Science (Cambridge), 2018, 9(12): 3209–3214
48. Lv F, Guo X, Wu H, Li H, Tang B, Yu C J, Hao E H, Jiao L J. Direct sulfonylation of BODIPY dyes with sodiumsulfinates through oxidative radical hydrogen substitution at the a-position. Chemical Communications, 2020, 56(99): 15577–15580
49. Liu J, Sun Y Q, Huo Y Y, Zhang H X, Wang L F, Zhang P, Song D, Shi Y W, Guo W. Simultaneous fluorescence sensing of Cys and GSH from different emission channels. Journal of the American Chemical Society, 2014, 136(2): 574–577
50. Fu X L, Chen X G, Li H, Feng W, Song Q H. Quinolone-based fluorescent probe for distinguishing detection of Cys and GSH

through different fluorescence channels. New Journal of Chemistry, 2020, 44(32): 13781–13787

51. Li H L, Peng W, Feng W P, Wang Y X, Chen G F, Wang S X, Li S H, Li H F, Wang K R, Zhang J C. A novel dual-emission fluorescent probe for simultaneous detection of H_2S and GSH. Chemical Communications, 2016, 52(25): 4628–4631
52. Li J, Yin C X, Zhang Y B, Yue Y K, Chao J B, Huo F J. High selective distinguishable detection GSH and H_2S based on steric configuration of molecular *in vivo*. Dyes and Pigments, 2020, 172: 107826
53. Zhao X X, He F R, Dai Y P, Ma F L, Qi Z J. A single fluorescent probe for one- and two-photon imaging hydrogen sulfide and hydrogen polysulfides with different fluorescence signals. Dyes and Pigments, 2020, 172: 107818
54. Li M Y, Cui P C, Li K, Feng J H, Zou M M, Yu X Q. Dual-site fluorescent probe for highly selective and sensitive detection of sulfite and biothiols. Chinese Chemical Letters, 2018, 29(6): 992–994
55. Wu X Y, Wang Y, Liu Y H, Yu X Q. Dual-site lysosome-targeted fluorescent probe for separate detection of endogenous biothiols and SO_2 in living Cells. Journal of Materials Chemistry. B, Materials for Biology and Medicine, 2018, 6(25): 4232–4238
56. Li Y, Liu W M, Zhang H Y, Wang M Q, Wu J S, Ge J C, Wang P F. Dual emission channels for simultaneous sensing Cys and Hcy in living cells. Chemistry, an Asian Journal, 2017, 12(16): 2098–2103
57. Chen W Q, Yue X X, Zhang H, Li W X, Zhang L L, Xiao Q, Huang C S, Sheng J R, Song X Z. Simultaneous detection of glutathione and hydrogen polysulfides from different emission channels. Analytical Chemistry, 2017, 89(23): 12984–12991
58. Yang X P, Liu W Y, Tang J, Li P, Weng H B, Ye Y, Xian M, Tang B, Zhao Y F. A multi-signal mitochondria-targeted fluorescent probe for real-time visualization of cysteine metabolism in living cells and animals. Chemical Communications, 2018, 54(81): 11387–11390
59. Zhao F F, Zha Z Y, Tang J, Zhang B B, Yang X P, Song X Z, Ye Y. A bond energy transfer based difunctional fluorescent sensor for Cys and bisulfite. Talanta, 2020, 214: 120884
60. Yin C X, Yu T, Gan Y B, Zhou L, Liu M L, Zhang Y Y, Li H T, Yin P, Yao S Z. A novel fluorescent probe with dual-sites for simultaneously monitoring metabolisms of cysteine in living cells and zebrafishes. Spectrochimica Acta. Part A: Molecular and Biomolecular Spectroscopy, 2020, 241: 118602
61. Yin J L, Ma Y Y, Li G H, Peng M, Lin W Y. A versatile small-molecule fluorescence scaffold: carbazole derivatives for bioimaging. Coordination Chemistry Reviews, 2020, 412: 213257
62. Zhu H, Fan J L, Du J J, Peng X J. Fluorescent probes for sensing and imaging within specific cellular organelles. Accounts of Chemical Research, 2016, 49(10): 2115–2126
63. Niu H W, Tang J, Zhua X F, Li Z P, Zhang Y R, Ye Y, Zhao Y F. Three-channel fluorescent probe to image mitochondrial stress. Chemical Communications, 2020, 56(56): 7710–7713
64. Dou K, Fu Q, Chen G, Yu F B, Liu Y X, Cao Z P, Li G L, Zhao X N, Xia L, Chen L X, Wang H, You J. A novel dual-ratiometric-response fluorescent probe for SO_2/ClO^- detection in cells and *in vivo* and its application in exploring the dichotomous role of SO_2 under the ClO^- induced oxidative stress. Biomaterials, 2017, 133: 82–93
65. Dou K, Guang C, Yu F B, Sun Z W, Li G L, Zhao X N, Chen L X, You J M. A two-photon ratiometric fluorescent probe for the synergistic detection of mitochondrial SO_2/HClO crosstalk in cells and *in vivo*. Journal of Materials Chemistry. B, Materials for Biology and Medicine, 2017, 5(42): 8389–8398
66. Yang L, Zhang Y, Ren X J, Wang B H, Yang Z G, Song X Z, Wang W. Fluorescent detection of dynamic H_2O_2/H_2S redox event in living cells and organisms. Analytical Chemistry, 2020, 92(6): 4387–4394
67. Velusamy N, Thirumalaivasan N, Bobba K N, Podder A, Wu S P, Bhuniya S. FRET-based dual channel fluorescent probe for detecting endogenous/exogenous H_2O_2/H_2S formation through multicolor images. Journal of Photochemistry and Photobiology. B, Biology, 2019, 191: 99–106
68. Yi L, Wei L, Wang R Y, Zhang C Y, Zhang J, Tan T W, Zhen X. A dual-response fluorescent probe reveals the H_2O_2-induced H_2S biogenesis through a cystathionine β-synthase pathway. Chemistry (Weinheim an der Bergstrasse, Germany), 2015, 21(43): 15167–15172
69. Jiao X Y, Xiao Y S, Li Y, Liang M W, Xie X L, Wang X, Tang B. Evaluating drug-induced liver injury and its remission via discrimination and imaging of HClO and H_2S with a two-photon fluorescent probe. Analytical Chemistry, 2018, 90(12): 7510–7516
70. Ren M G, Li Z H, Deng B B, Wang L, Lin W Y. Single fluorescent probe separately and continuously visualize H_2S and HClO in lysosomes with different fluorescence signals. Analytical Chemistry, 2019, 91(4): 2932–2938
71. Yue X X, Wang J P, Han J L, Wang B H, Song X Z. A dual-ratiometric fluorescent probe for individual and continuous detection of H_2S and HClO in living cells. Chemical Communications, 2020, 56(19): 2849–2852
72. Li Y, Xie X L, Yang X E, Li M M, Jiao X Y, Sun Y H, Wang X, Tang B. Two-photon fluorescent probe for revealing drug-induced hepatotoxicity via mapping fluctuation of peroxynitrite. Chemical Science (Cambridge), 2017, 8(5): 4006–4011
73. Wang N N, Yu X Y, Zhang K, Mirkin C A, Li J S. Upconversion nanoprobes for the ratiometric luminescent sensing of nitric oxide. Journal of the American Chemical Society, 2017, 139(36): 12354–12357
74. Fransen M, Nordgren M, Wang B, Apanasets O. Role of peroxisomes in ROS/RNS-metabolism: implications for human disease. Biochimica et Biophysica Acta, 2012, 1822(3): 1363–1373
75. Moldogazieva N T, Mokhosoev I M, Feldman N B, Lutsenko S V. ROS and RNS signaling: adaptive redox switches though oxidative/nitrosative protein modifications. Free Radical Research, 2018, 52(5): 507–543
76. Zhang P S, Li J, Li B W, Xu J S, Zeng F, Lv J, Wu S Z. A logic gate-based fluorescent sensor for detecting H_2S and NO in aqueous media and inside live cells. Chemical Communications, 2015, 51(21): 4414–4416
77. Chen X X, Niu L Y, Shao N, Yang Q Z. BODIPY-based fluorescent probe for dual-channel detection of nitric oxide and glutathione: visualization of cross-talk in living cells. Analytical Chemistry, 2019, 91(7): 4301–4306
78. Zhang J J, Chai X Z, He X P, Kim H J, Yoon J Y, Tian H. Fluorogenic probes for disease-relevant enzymes. Chemical Society

Reviews, 2019, 48(2): 683–722
79. Kim H M, Cho B R. Small-molecule two-photon probes for bioimaging applications. Chemical Reviews, 2015, 115(11): 5014–5055
80. Yuan L, Lin W Y, Xie Y N, Chen B, Zhu S S. Single fluorescent probe responds to H_2O_2, NO, and H_2O_2/NO with three different sets of fluorescence signals. Journal of the American Chemical Society, 2012, 134(2): 1305–1315
81. Wu Z, Liu M M, Liu Z C, Tian Y. Real-time imaging and simultaneous quantification of mitochondrial H_2O_2 and ATP in neurons with a single two-photon fluorescence lifetime-based probe. Journal of the American Chemical Society, 2020, 142(16): 7532–7541
82. Ou P, Zhang R, Liu Z, Tian X, Han G, Liu B, Hu Z, Zhang Z. Gasotransmitter Regulation of Phosphatase Activity in Live Cells Studied by Three-Channel Imaging Correlation. Angewandte Chemie International Edition, 2019, 131(8): 2283–2287
83. Fang Y, Shi W, Hu Y M, Li X H, Ma H M. A dual-function fluorescent probe for monitoring the degrees of hypoxia in living cells via the imaging of nitroreductase and adenosine triphosphate. Chemical Communications, 2018, 54(43): 5454–5457
84. Li Y H, Wang H, Li J H, Zheng J, Xu X H, Yang R H. Simultaneous intracellular β-D-glucosidase and phosphodiesterase I activities measurements based on a triple-signaling fluorescent probe. Analytical Chemistry, 2011, 83(4): 1268–1274
85. Fu L, Tian F F, Lai L, Liu Y, Harvey P D, Jiang F L. A ratiometric “two-in-one” fluorescent chemodosimeter for fluoride and hydrogen sulfide. Sensors and Actuators. B, Chemical, 2014, 193: 701–707